LIMITED CONVERGENCE IN AQUATIC CROCODYLIFORMES: SUPPLEMENTARY INFORMATION

ISAURE SCAVEZZONI AND VALENTIN FISCHER

CONTENTS

1. ABBREVIATIONS

BRLSI Bath: Bath Royal Literary and Scientific Institute, UK; **BRSMG** Bristol: Bristol City Museum and Art Gallery, UK; **GPIT** Tübingen: Geologisch–Paläontologisches Institut Tübingen, Germany; **GLAHM** Glasgow: Hunterian Museum and Art Gallery, UK; **MLP** La Plata: Museo de La Plata, Buenos Aires, Argentina; **LRM** Lyme: Lyme Regis Museum, UK; **MRAC** Tervuren: Musée Royal de l'Afrique Centrale, Belgium; **NHM UK** London: Natural History Museum, UK; **NJSM** Trenton: New Jersey State Museum, USA; **NKMB** Bamberg: Naturkunde-Museum Bamberg, Germany; **OCP DEK-GE** Khouribga: Office Chérifien des Phosphates, Direction de l'Exploitation de Khouribga, Geologie-Exploitation, Khouribga, Morocco; **PMU** Uppsala: Evolutionsmuseet – Uppsala universitet, Sweden; **RBINS** Brussels: Royal Belgian Institute of Natural Sciences, Belgium; **SMNS** Stuttgart: Staatliches Museum für Naturkunde, Germany; **UF/IGM** Gainesville: **UF**, Florida Museum of Natural History, University of Florida, USA / **IGM**, Museo Geológico, at the Instituto Nacional de Investigaciones en Geociencias, Minería y Quimica, Bogotá, Colombia; **UJF** Grenoble; Joseph Fourier University, France; **YPM** New Haven: Yale Peabody Museum, USA.

SCR: 'Sur Combe Ronde', specimens housed at the Jurassica Museum (Switzerland).

2. List of specimens

Inventory number	Taxa	Ilium	Ischium	Pubis	Femur	Scapula	Coracoid	Humerus
RBINS 18374	*Mecistops cataphractus*	**1**	**1**	**1**	**1**	**1**	**1**	**1**
LRM 2021/45	*Turnersuchus hingleyae*					1		
MLP 72-IV-7-1	*Cricosaurus araucanensis*	1						
SMNS 8203	*Dakosaurus maximus*				1			1
UJF–ID.11846m	*Geosaurus lapparenti*							1
NHMUK PV R 1230	*Geosaurus giganteus*	1		1				
NHMUK PV R 4763	*'Metriorhynchus' brachyrhynchus*	1	1		1			
NHMUK PV R 3804	*'Metriorhynchus' brachyrhynchus*	**1**	**1**	**1**	**1**			
BRLSI M.1410	*Pelagosaurus typus*		1					
BRLSI M.1417:1	*Pelagosaurus typus*	1						
BRLSI M.1420	*Pelagosaurus typus*			1				
NHMUK PV R 2618	*Suchodus durobrivensis*	1		1	1			
GLAHM V950	*'Thalattosuchus' superciliosus*		1					
GLAHM V960	*'Thalattosuchus' superciliosus*		1^{x2}	1	1			
GLAHM V1005	*'Thalattosuchus' superciliosus*	**1**	**1**	**1**	**1**		1	
GLAHM V1016	*'Thalattosuchus' superciliosus*							1
GLAHM V1143	*Thalattosuchus superciliosus*						**1**	**1**
GLAHM V1146	*'Thalattosuchus' superciliosus*	1				**1**	**1**	**1**
NHMUK PV R 1530	*Thalattosuchus superciliosus*	**1**	**1**	1	1		**1**	
NHMUK PV R 2032	*Thalattosuchus superciliosus*				1			**1**
NHMUK PV R 2054	*Thalattosuchus superciliosus*	1	1	**1**	**1**			
PMU 35988	*Thalattosuchus superciliosus*					**1**	1	
BRSMG Cd7203	*Torvoneustes carpenteri*		1		1			1
GLAHM V972	*Tyrannoneustes lythrodectikos*	1						
GLAHM V1145	*Tyrannoneustes lythrodectikos*	1			1		1	1
NHMUK PV R 3806	*Charitomenosuchus leedsi*	**1**	**1**	**1**	**1**	**1**	**1**	**1**
NHMUK PV R 3168	*Lemmysuchus obtusidens*	**1**	**1**	**1**	**1**	**1**		**1**
NHMUK PV R 3169	*Neosteneosaurus edwardsi*						**1**	
SMNS 81608	*Machimosaurus hugii*			1	1			
NHMUK PV R 5703	*Macrospondylus bollensis*			1				
NHMUK PV R 2617	*Mycterosuchus nasutus*					**1**	**1**	**1**
NHMUK PV R 3169	*Neosteneosaurus edwardsi*				1		1	
NHMUK PV R 3701	*Neosteneosaurus edwardsi*		**1**	**1**		**1**	**1**	**1**
NHMUK PV R 2076	*Neosteneosaurus edwardsi*	**1**		1	**1**			
NHMUK PV R 2865	*Neosteneosaurus edwardsi*		1		1			
SCR010-374	*Proexochokefalos cf. bouchardi*	1	1					1
SCR010-312	*Sericodon jugleri*	1	1		1			1
UF/IGM 38	*Acherontisuchus guajiraensis*	1	1					
MRAC 1806		1						
MRAC 1809						**1**		
MRAC 1811	*Congosaurus bequaerti*						**1**	
MRAC 1813								**1**
MRAC 1817					1			
YPM VP.000753	*Hyposaurus natator*	1			1			
YPM VP.00985	*Hyposaurus natator*						1	1
NJSM 23368	*Hyposaurus natator*	**1**	**1**	**1**	**1**	**1**	**1**	**1**
Total		22	19	17	23	10	14	17

Table S 1. List of taxa used in our landmark analyses. Numbers in bold indicate which bones were used in the combined analysis.

3. Reconstructions

Obvious defect portions such as cracks or shifted portions were repaired in Blender using the overall shape of the surrounding walls as reference. Missing portions such as broken extremities were repaired in Blender using the best preserved phylogenetically closest (based on the works of Jouve and Jalil [2020], Johnson et al. [2020], Young et al. [2020], Wilberg et al. [2023]) taxon for each incomplete specimen (see Table 2). Cut out portions from reference taxa were then adapted in size and thickness before being sutured to the incomplete specimen.

Broken specimen	Bone type	Reference specimen
Congosaurus bequaerti MRAC 1809	Scapula	*Hyposaurus natator* NJSM 23368
Charitomenosuchus leedsi NHMUK PV R 3806	Ischium	*Neosteneosaurus edwardsi* NHMUK PV R 2865
Mycterosuchus nasutus NHMUK PV R 2617	Coracoid	*Charitomenosuchus leedsi* NHMUK PV R 3806
Dakosaurus maximus SMNS 8203	Femur	*Tyrannoneustes lythrodectikos* GLAHM V1145
Geosaurus lapparenti UJF–ID.11846m	L Humerus	*Geosaurus lapparenti* UJF–ID.11846m R Humerus
Geosaurus lapparenti UJF–ID.11846n	Femur	*Tyrannoneustes lythrodectikos* GLAHM V1145
Lemmysuchus obtusidens NHMUK PV R 3168	Humerus	*Neosteneosaurus edwardsi* NHMUK PV R 3701
Lemmysuchus obtusidens NHMUK PV R 3168	Pubis	*Neosteneosaurus edwardsi* NHMUK PV R 2076
Machimosaurus hugii SMNS 81608	L Pubis	*Neosteneosaurus edwardsi* NHMUK PV R 2076 & *Machimosaurus hugii* SMNS 81608 R Pubis
'Metriorhynchus' brachyrhynchus NHMUK PV R 3804	Ischium	*'Metriorhynchus' brachyrhynchus* NHMUK PV R 4763 & *Tyrannoneustes lythrodectikos* GLAHM V972
Neosteneosaurus edwardsi NHMUK PV R 3701	Coracoid	*Charitomenosuchus leedsi* NHMUK PV R 3806
Neosteneosaurus edwardsi NHMUK PV R 3169	Coracoid	*Neosteneosaurus edwardsi* NHMUK PV R 3701
Neosteneosaurus edwardsi NHMUK PV R 3701	Ischium	*Neosteneosaurus edwardsi* NHMUK PV R 2865
Pelagosaurus typus BRLSI M.1417:1	Ilium	*Pelagosaurus typus* SMNS 17758
Pelagosaurus typus BRLSI M.1410	Ischium	*Pelagosaurus typus* BRLSI M.1424
Pelagosaurus typus BRLSI M.1420	Pubis	*Pelagosaurus typus* SMNS 17758
'Thalattosuchus' superciliosus GLAHM V950	Ischium	*'Thalattosuchus' superciliosus* GLAHM V1005
'Thalattosuchus' superciliosus GLAHM V960	Ischium 1	*'Thalattosuchus' superciliosus* GLAHM V1005
'Thalattosuchus' superciliosus GLAHM V960	Ischium 2	*Thalattosuchus superciliosus* NHMUK PV R 2054
'Thalattosuchus' superciliosus GLAHM V1005	Coracoid	*Tyrannoneustes lythrodectikos* GLAHM V1145
'Thalattosuchus' superciliosus GLAHM V1005	Ischium	*'Thalattosuchus' superciliosus* GLAHM V1005 R ischium *'Thalattosuchus' superciliosus* GLAHM V960
Thalattosuchus superciliosus NHMUK PV R 2054	Ischium	*Thalattosuchus superciliosus* NHMUK PV R 1530
Thalattosuchus superciliosus NHMUK PV R 1530	Coracoid	*'Thalattosuchus' superciliosus* GLAHM V1005
Thalattosuchus superciliosus PMU 35988	Coracoid	*'Thalattosuchus' superciliosus* GLAHM V1005

TABLE S 2. List of repaired taxa with their reference.

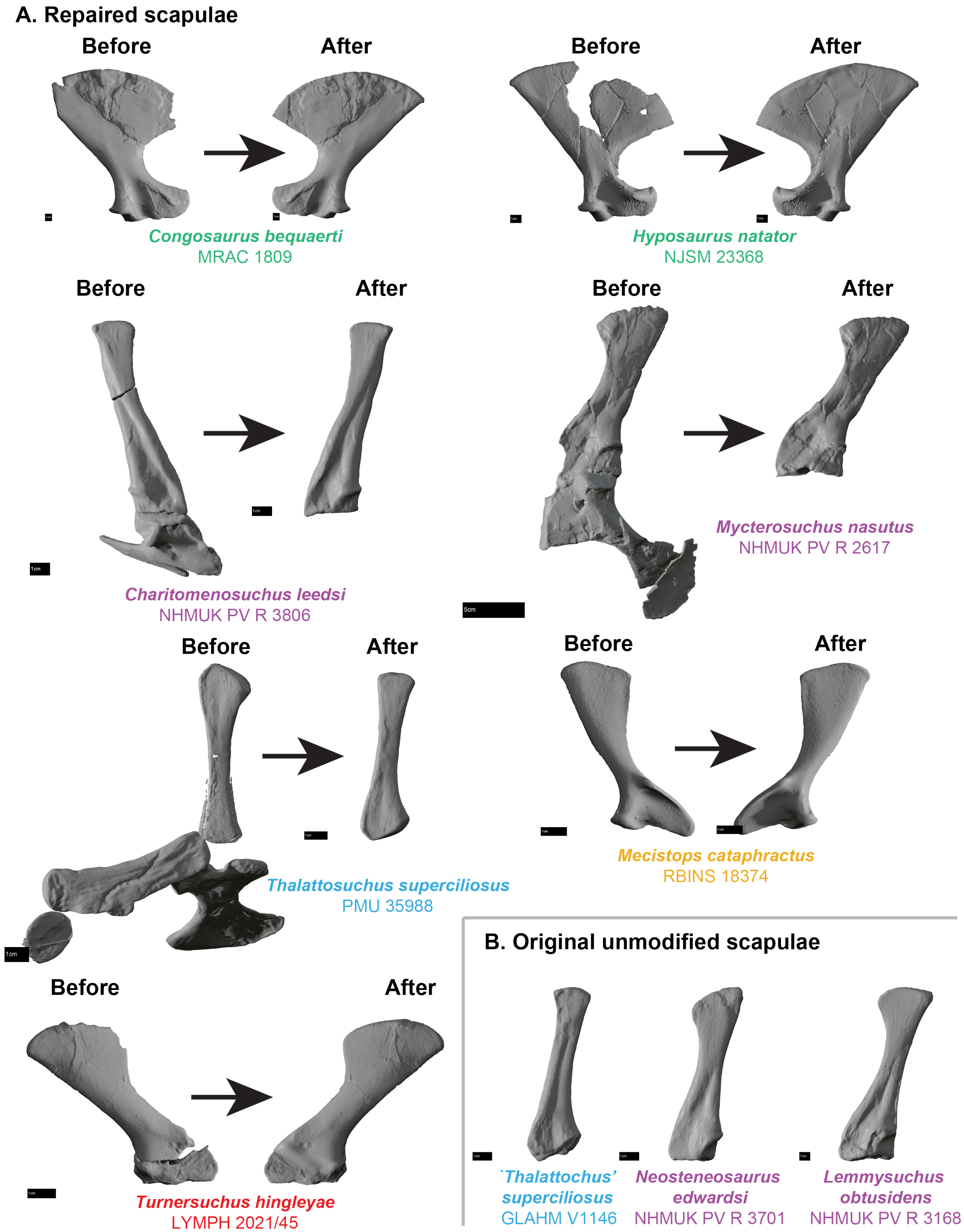

FIGURE S 1. Scapulae 3D models before and after. **A.** Repaired scapulae; **B.** Original unmodified scapulae.

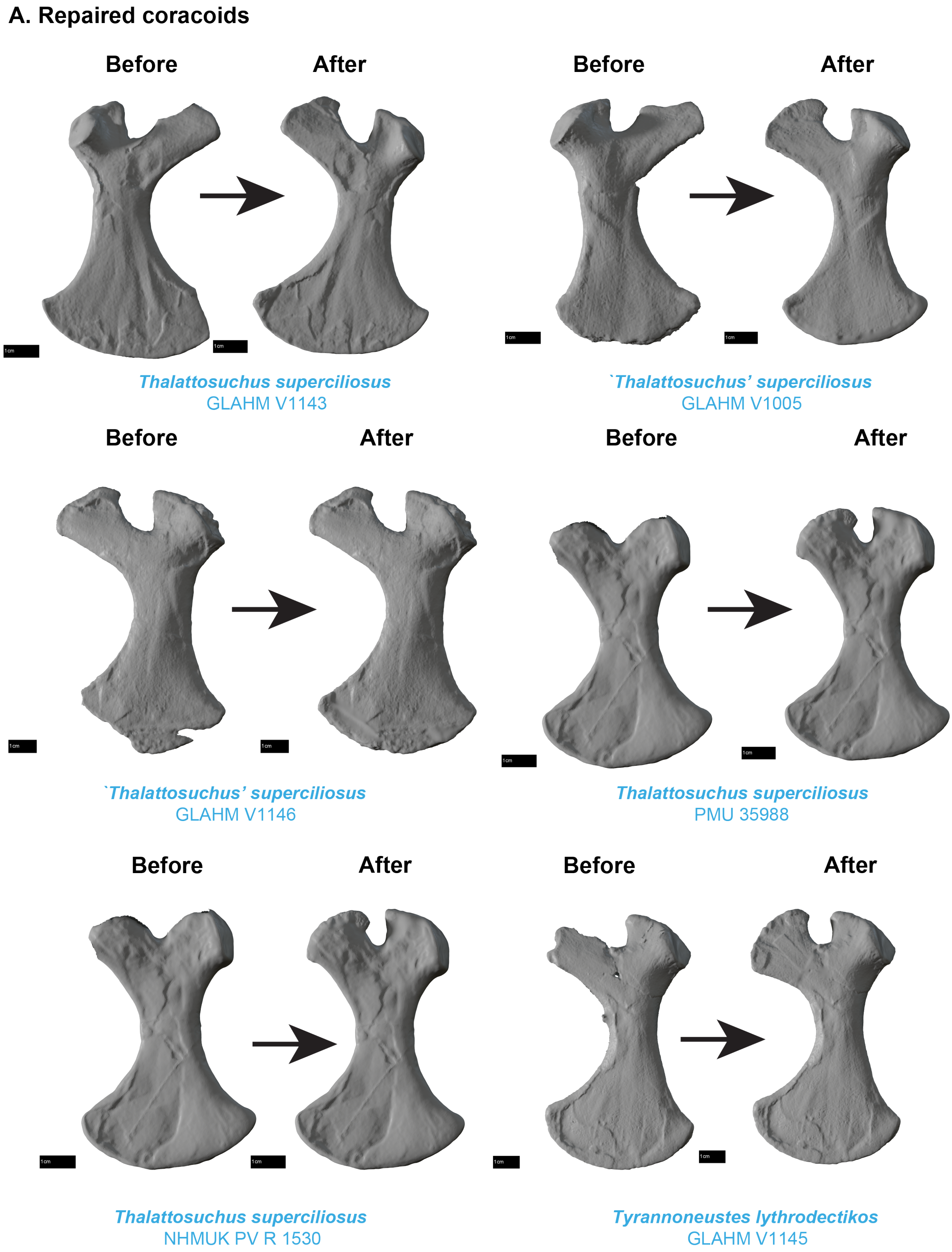

FIGURE S 2. Coracoids 3D models before and after. **A.** Repaired coracoids.

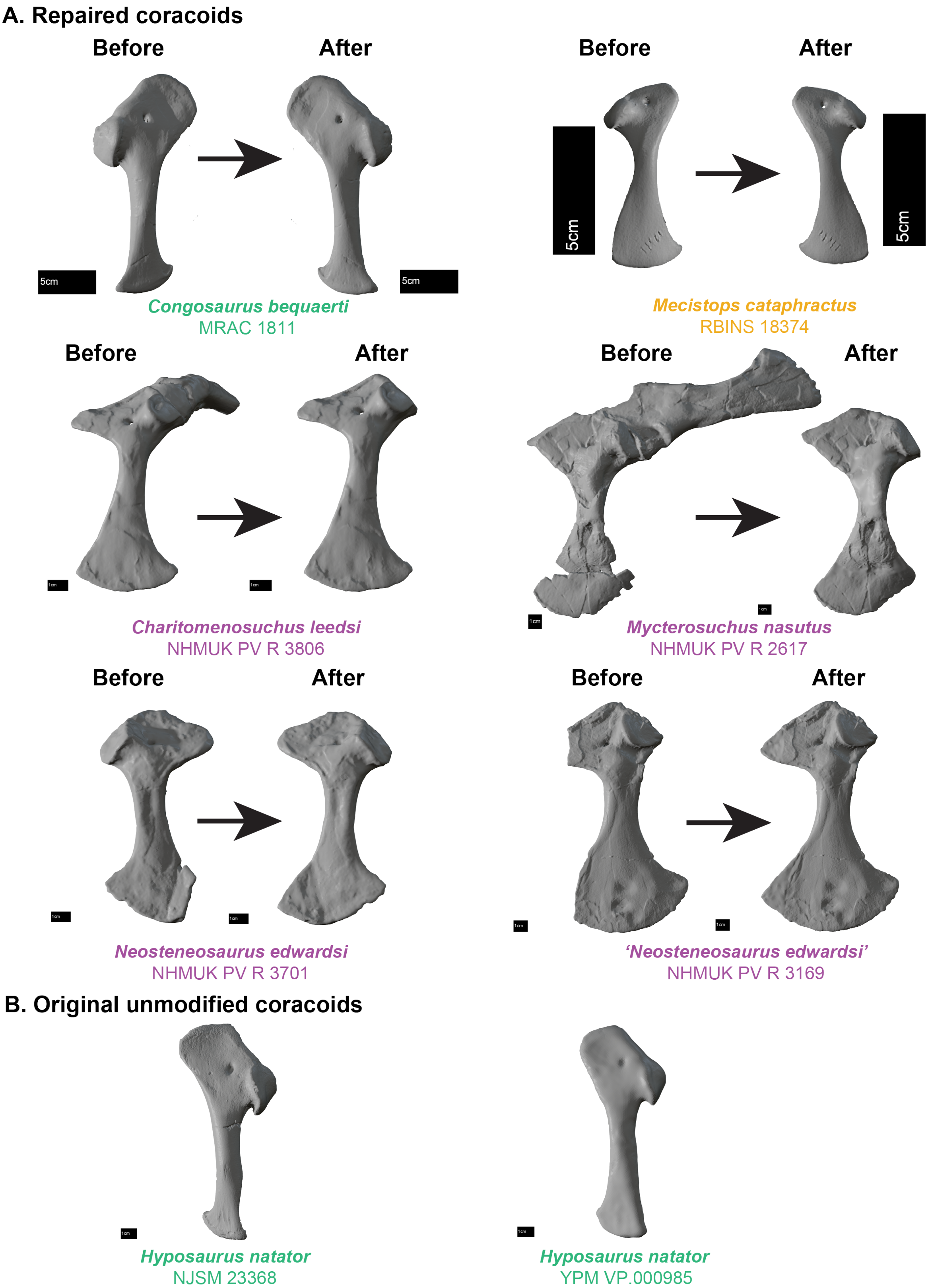

FIGURE S 3. Coracoids 3D models before and after. **A.** Repaired coracoids; **B.** Original unmodified coracoids.

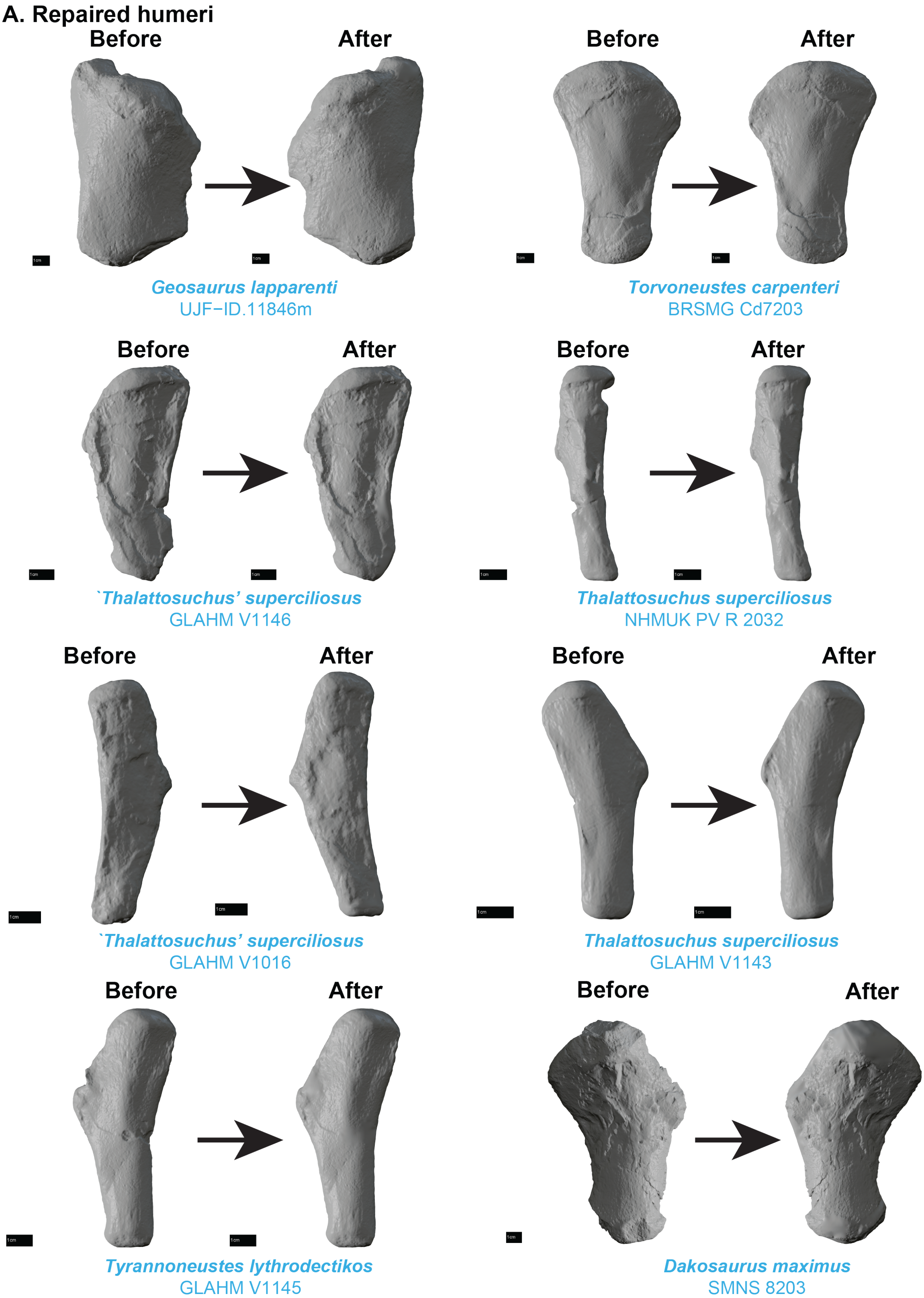

FIGURE S 4. Humeri 3D models before and after. **A.** Repaired humeri.

A. Repaired humeri

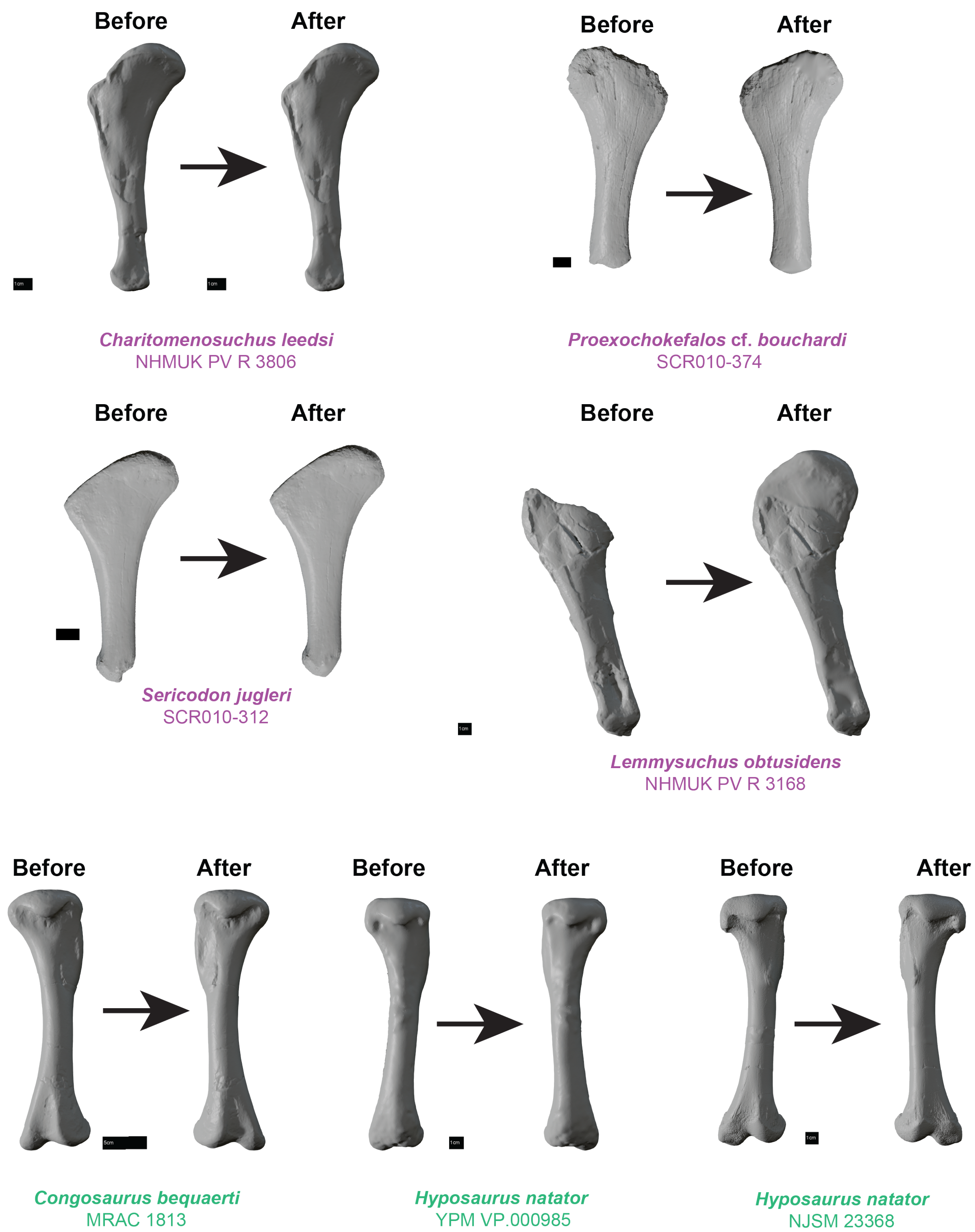

FIGURE S 5. Humeri 3D models before and after. **A.** Repaired humeri.

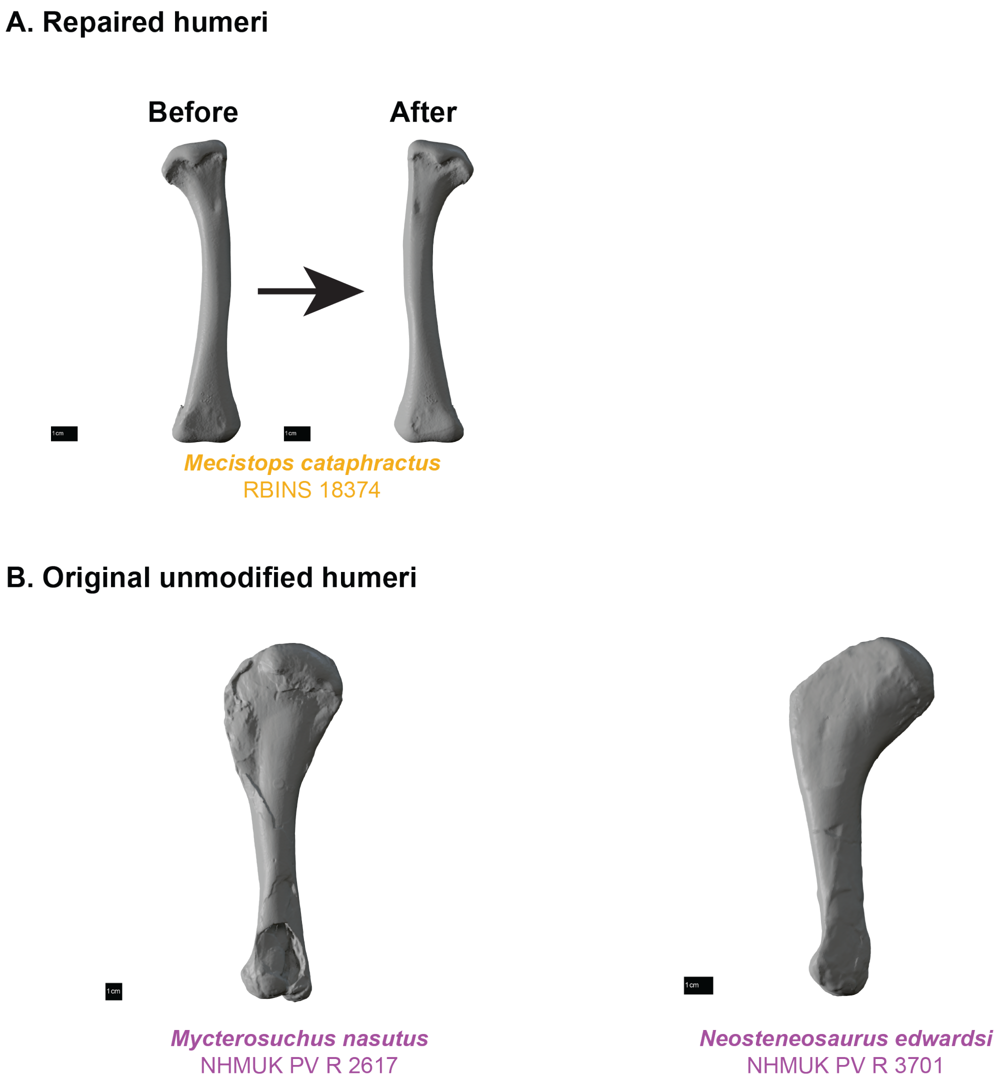

FIGURE S 6. Humeri 3D models before and after. **A.** Repaired humeri; **B.** Original unmodified humeri.

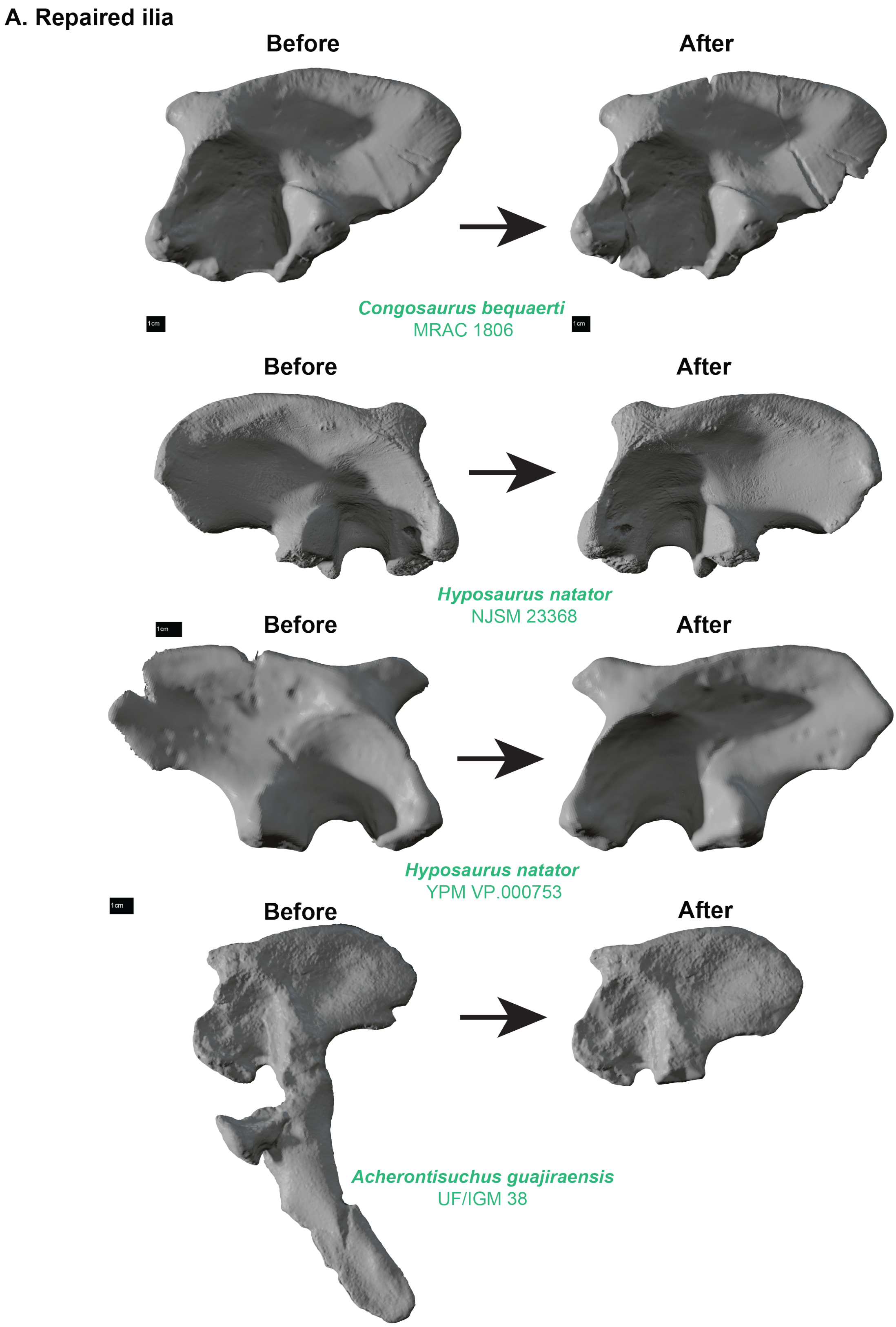

FIGURE S 7. Ilia 3D models before and after. **A.** Repaired ilia.

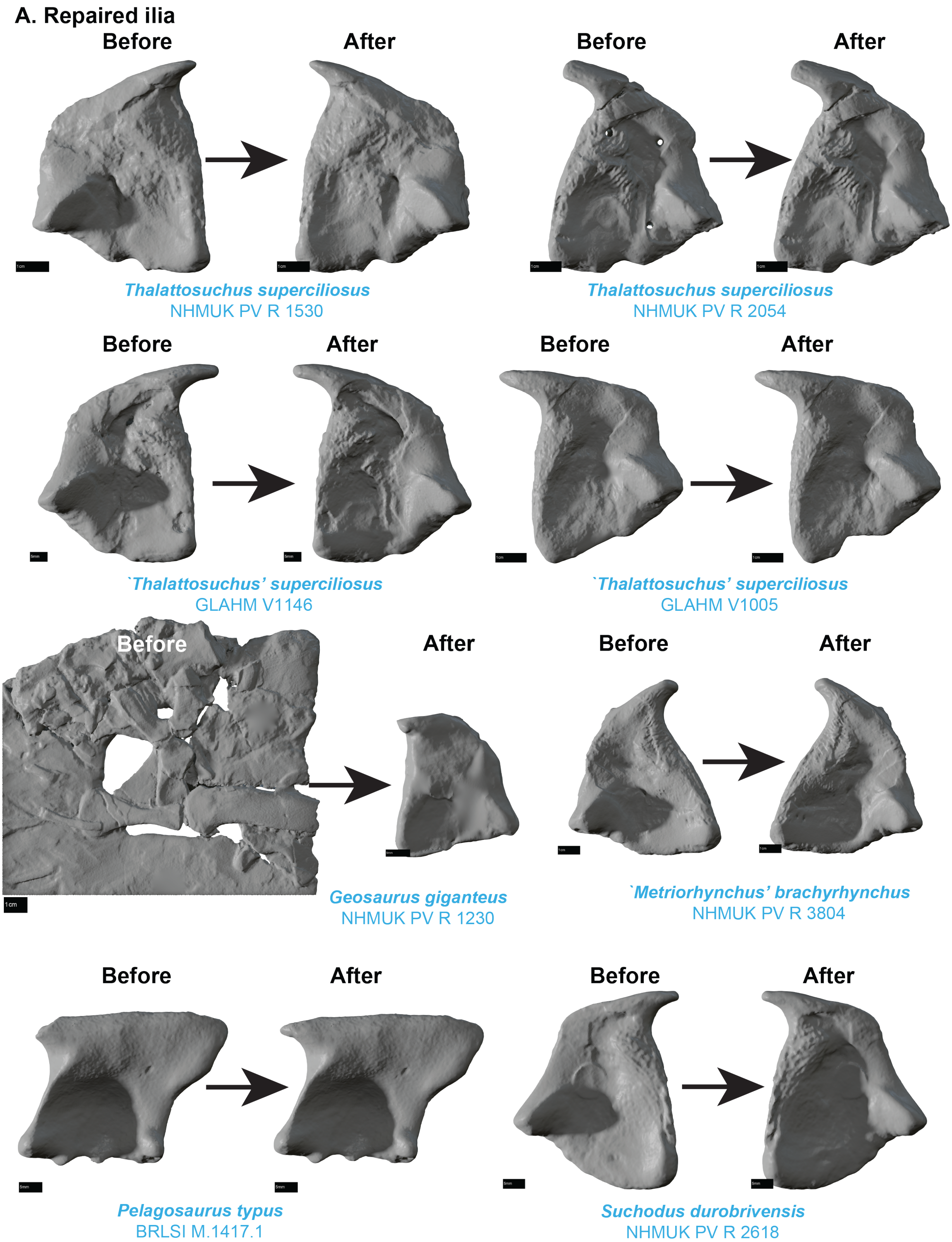

FIGURE S 8. Ilia 3D models before and after. **A.** Repaired ilia.

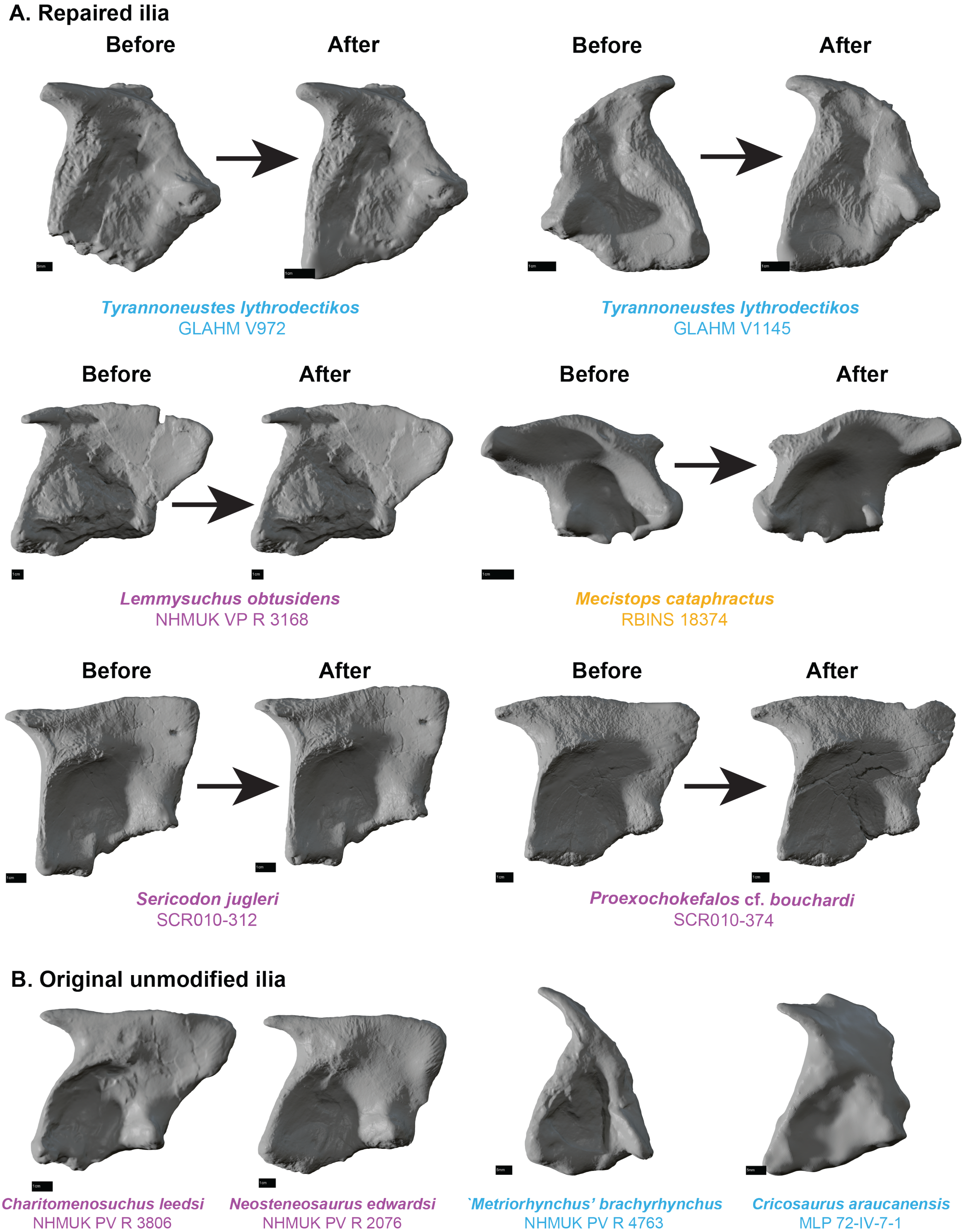

FIGURE S 9. Ilia 3D models before and after. **A.** Repaired ilia; **B.** Original unmodified ilia.

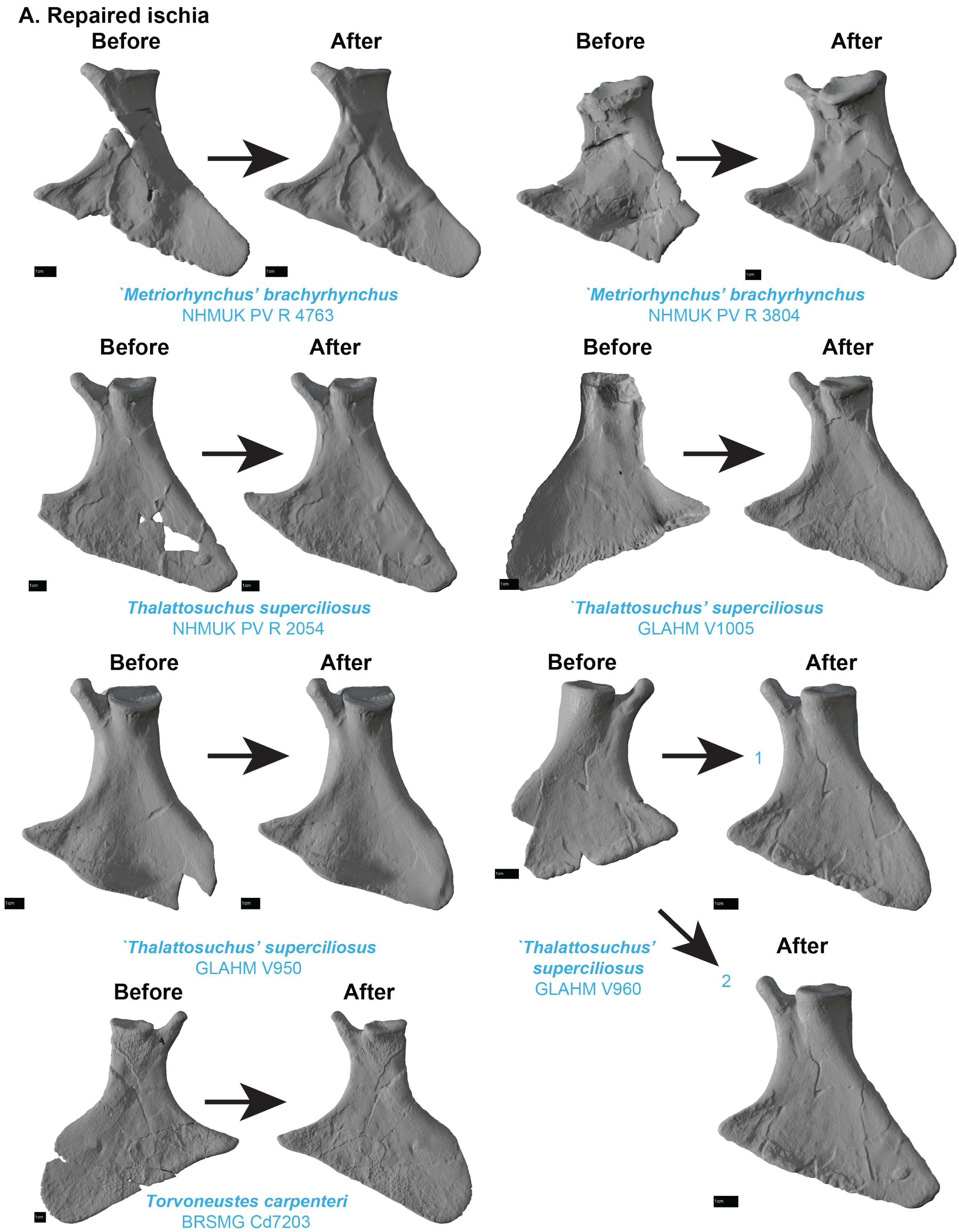

FIGURE S 10. Ischia 3D models before and after. **A.** Repaired ischia.

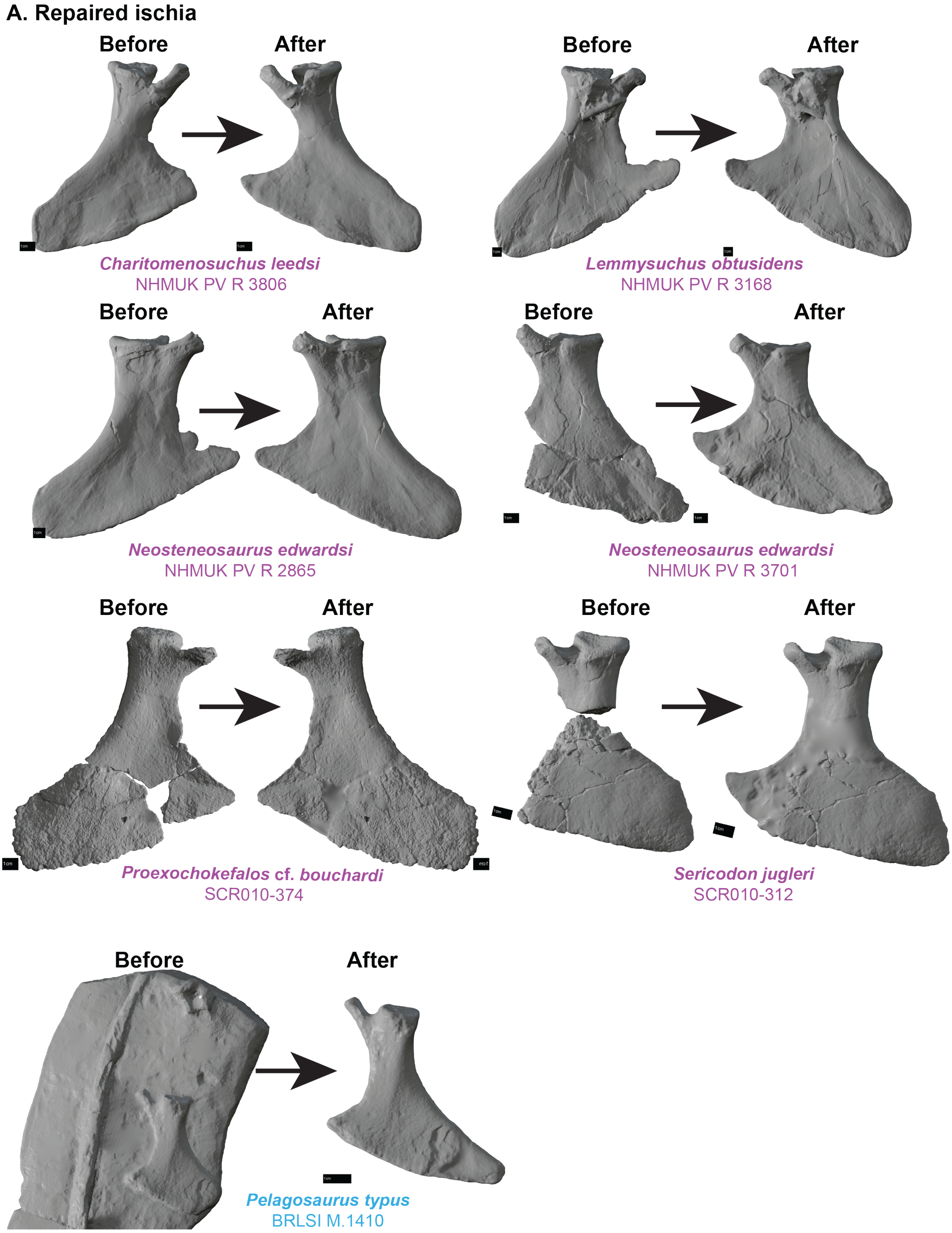

FIGURE S 11. Ischia 3D models before and after. **A.** Repaired ischia.

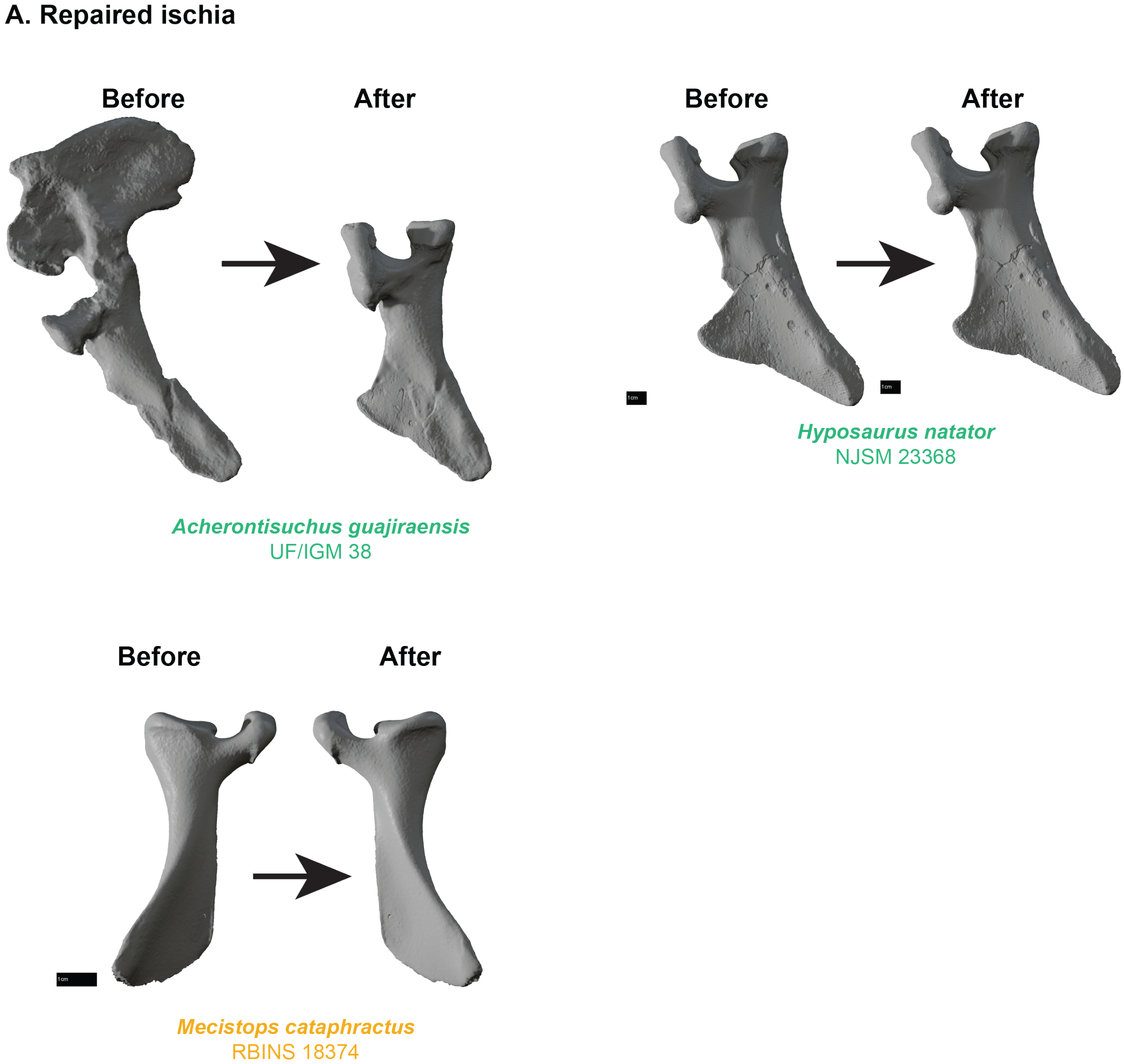

FIGURE S 12. Ischia 3D models before and after. **A.** Repaired ischia.

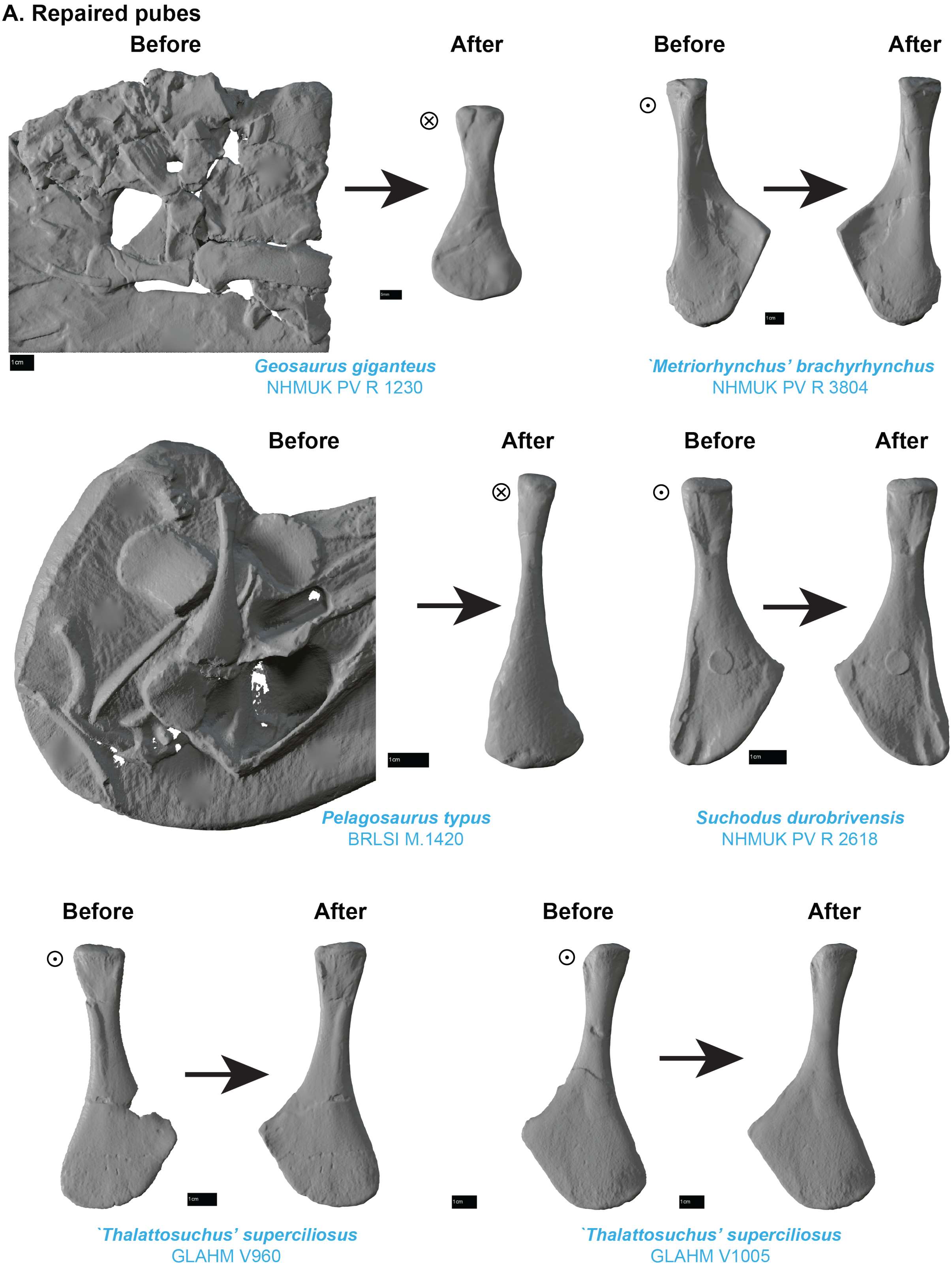

FIGURE S 13. Pubes 3D models before and after. **A.** Repaired pubes. Target indicates anterior. Cross indicates posterior.

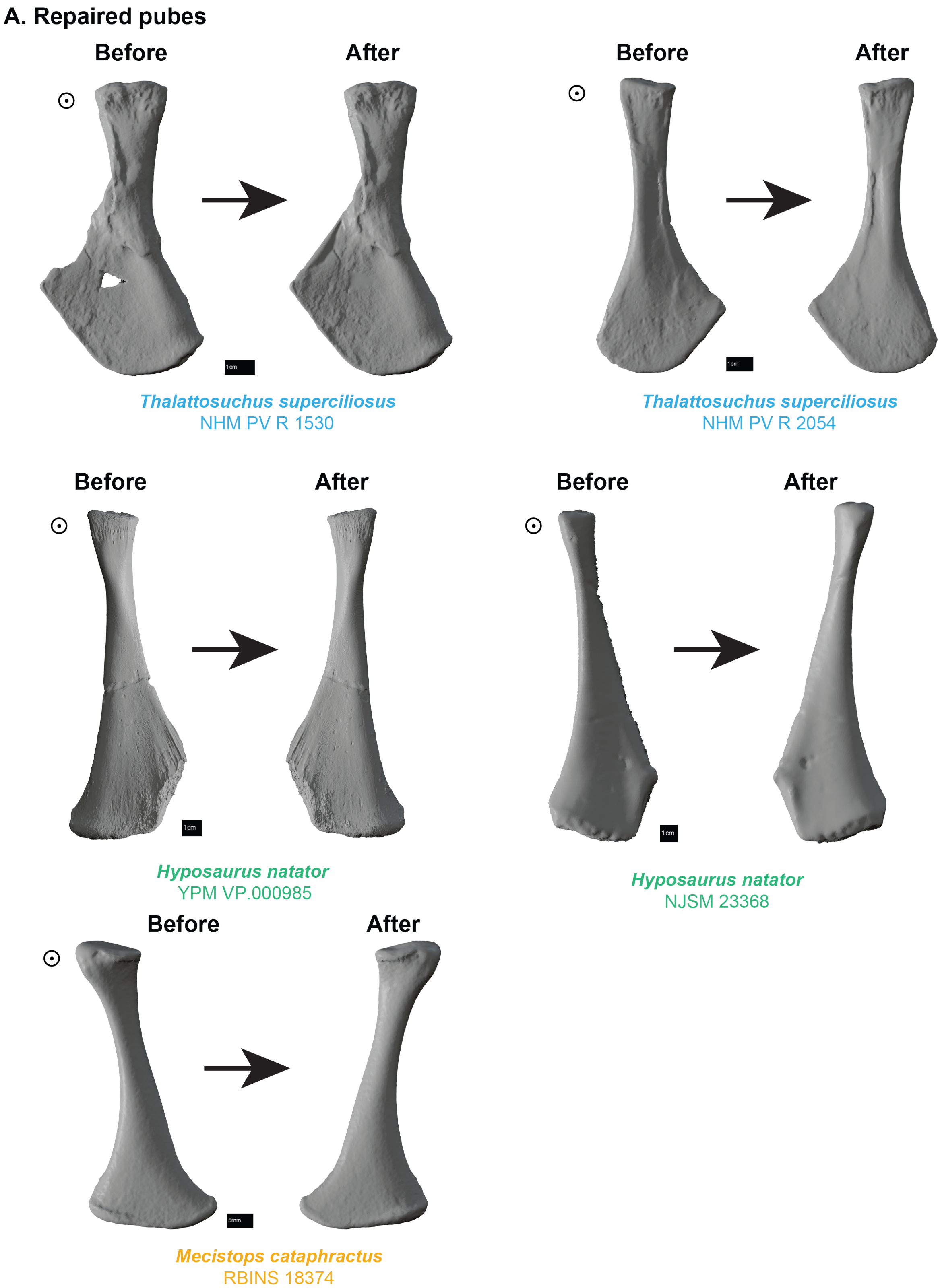

FIGURE S 14. Pubes 3D models before and after. **A.** Repaired pubes. Target indicates anterior. Cross indicates posterior.

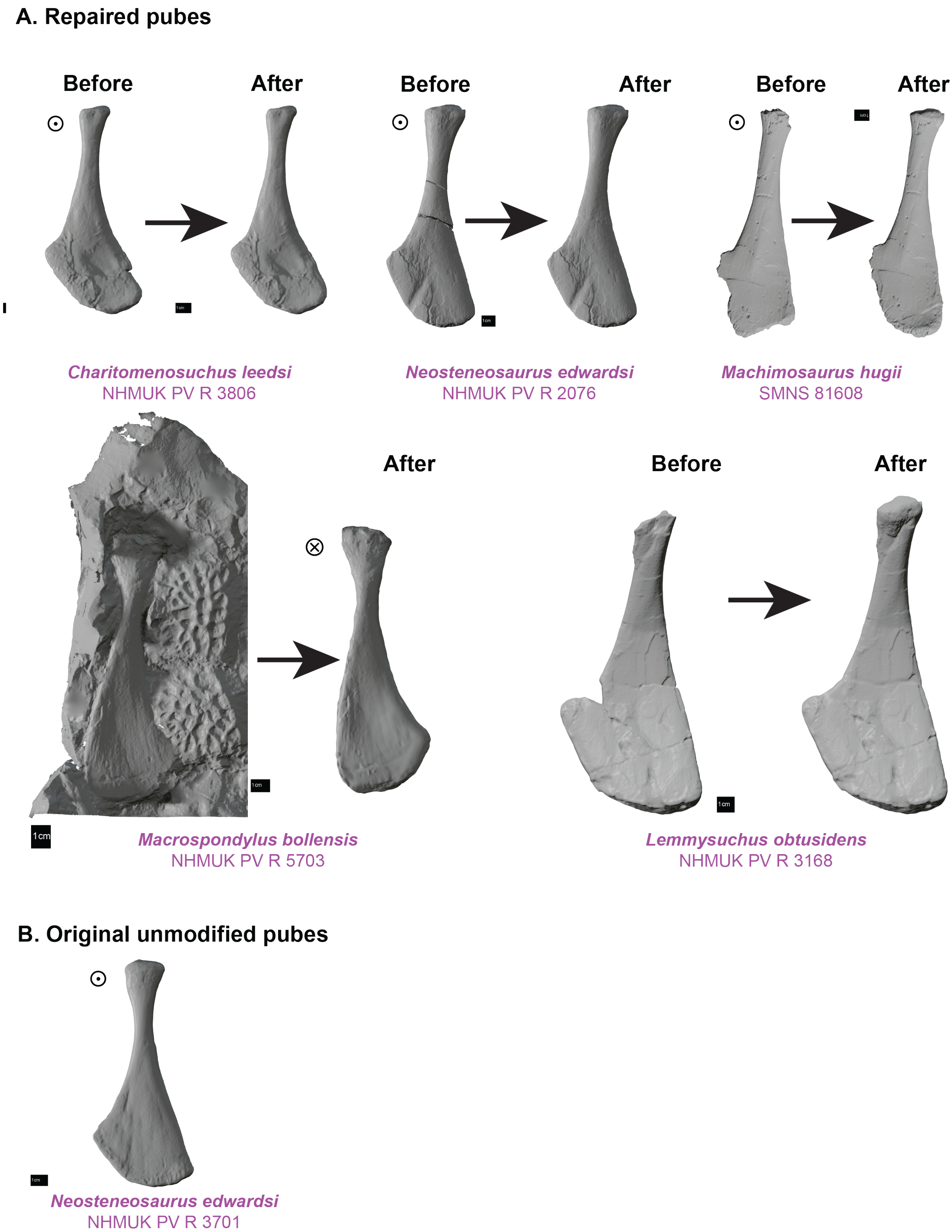

FIGURE S 15. Pubes 3D models before and after. **A.** Repaired pubes; **B.** Original unmodified pubes.

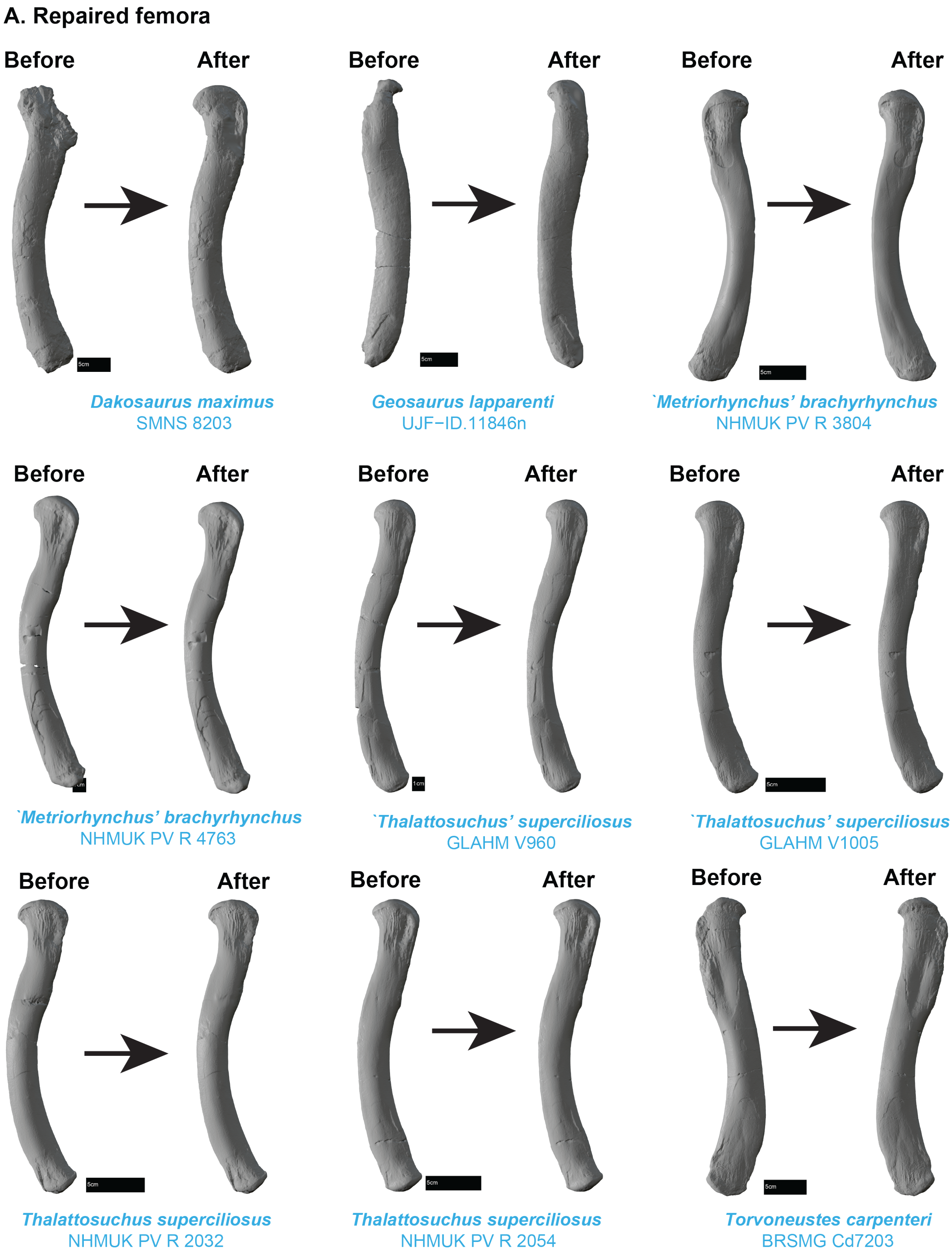

FIGURE S 16. Femora 3D models before and after. **A.** Repaired femora.

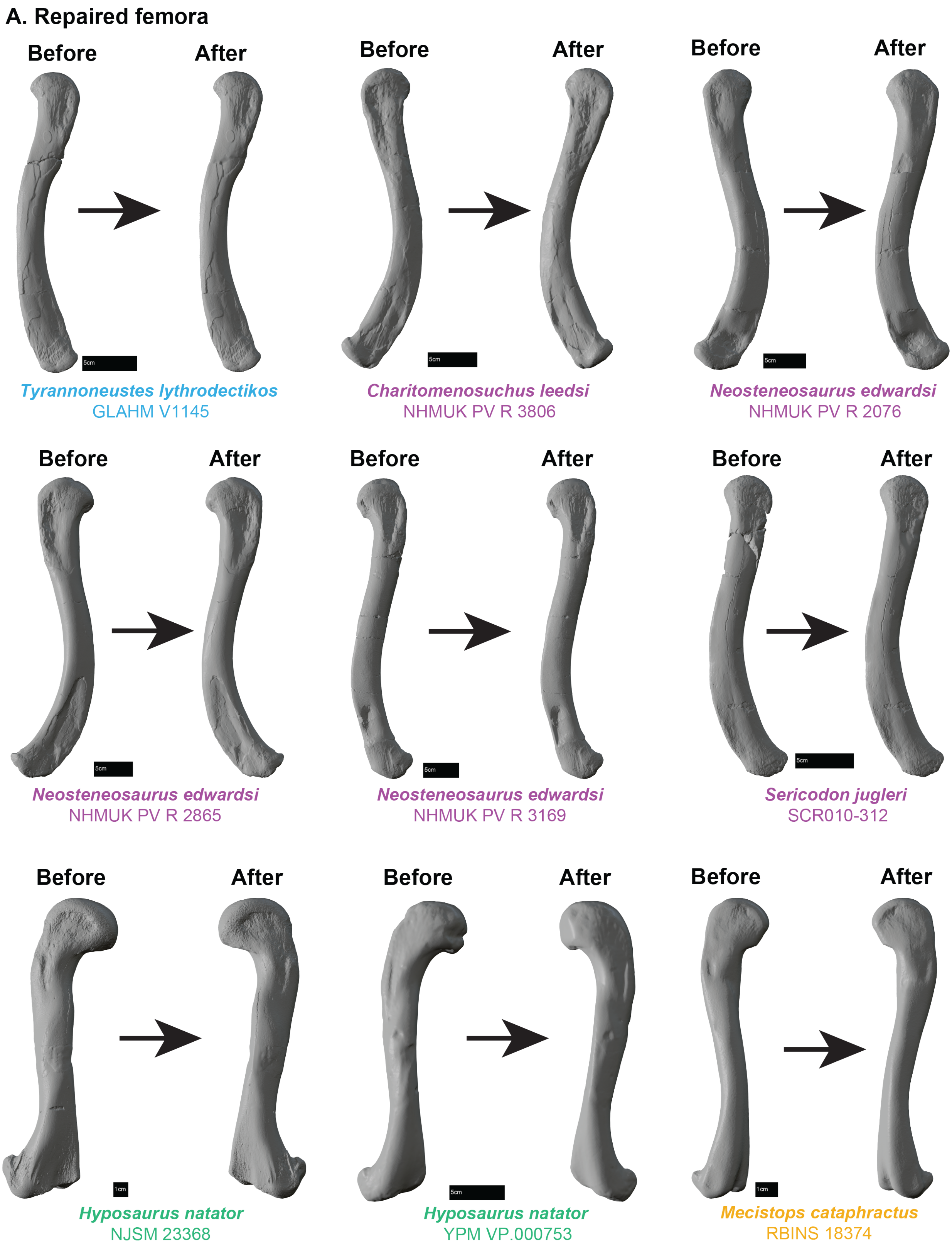

FIGURE S 17. Femora 3D models before and after. **A.** Repaired femora.

B. Original unmodified femora

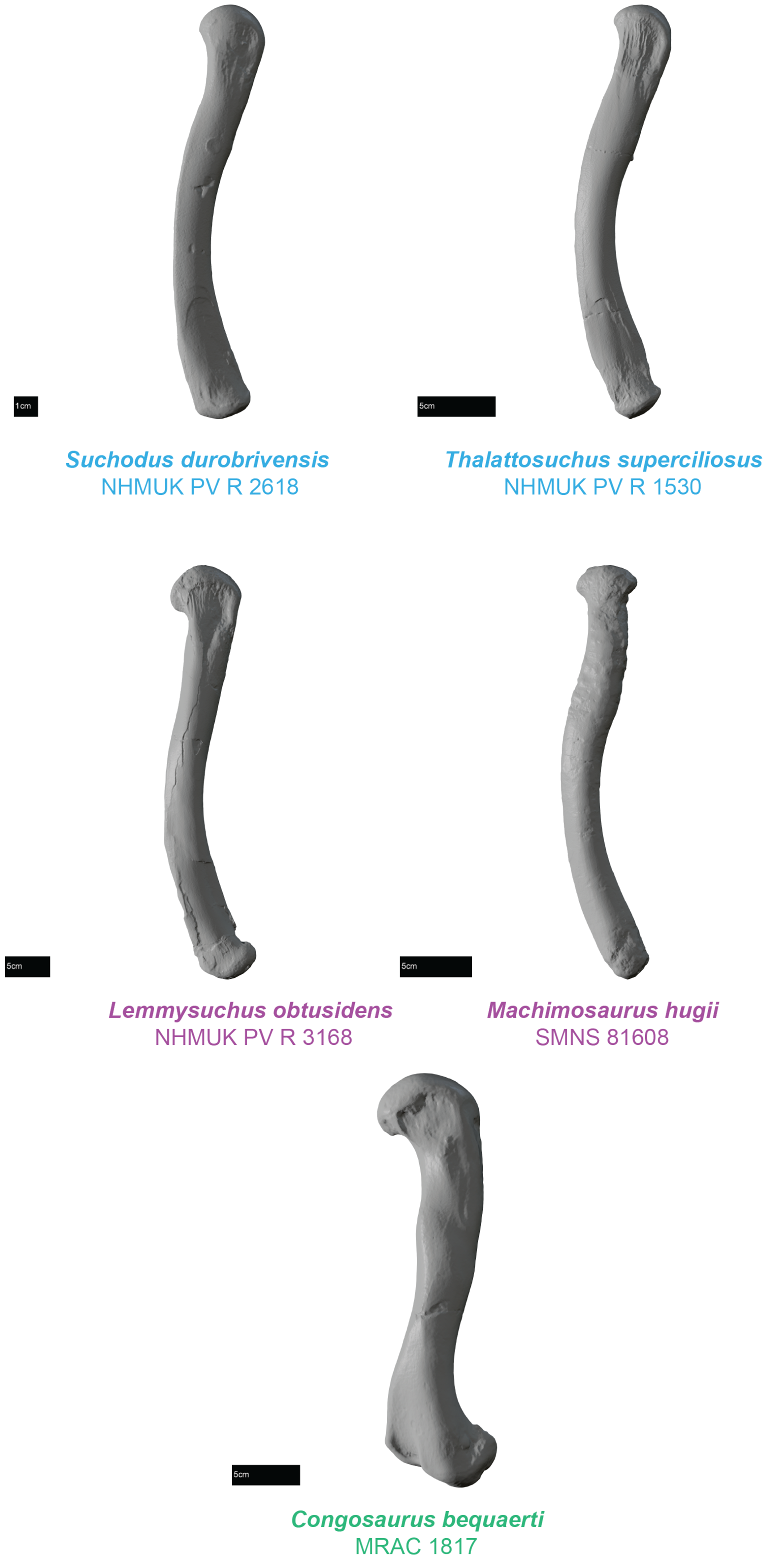

FIGURE S 18. Femora 3D models. **B.** Original unmodified femora.

4. Statistical analyses

Bone	K_{mult}	p-value
Pelvic combined	0.3064	**0.003***
Thoracic combined	0.3665	**0.001***
Scapula	0.5543	**0.001***
Coracoid	0.4969	**0.001***
Humerus	0.3472	**0.001***
Ilium	0.5642	**0.001***
Ischium	0.4562	**0.002***
Pubis	0.2943	**0.003***
Femur	0.4595	**0.001***

TABLE S 3. Values of Kmult for each bone of the entire dataset (Thalattosuchia–Dyrosauridea–Crocodylia). Significant p-value $< 0.005^*$ (α=0.005).

Bone	K_{mult}	p-value
Scapula	0.6319	**0.002** *
Coracoid	0.4101	**0.001** *
Humerus	0.4897	**0.001** *
Ilium	0.7648	**0.001***
Ischium	0.3299	0.023
Pubis	0.395	0.02
Femur	0.3302	**0.001** *

TABLE S 4. Values of Kmult for each bone for Thalattosuchia. Significant p-value $< 0.005^*$ (α=0.005).

TAXA 1 – TAXA 2	**Scapula Ct1**	**p-value**
Congosaurus bequaerti–Lemmysuchus obtusidens	-1.178640821	0.465
Mycterosuchus nasutus–Mecistops cataphractus	-0.908551875	**0.036** *
Mecistops cataphractus–Congosaurus bequaerti	-3.792548894	0.247
Thalattosuchus superciliosus–Hyposaurus natator	-0.980952356	0.424
Charitomenosuchus leedsi–Thalattosuchus superciliosus	-0.148915652	0.708
Neosteneosaurus edwardsi–Mycterosuchus nasutus	-0.29638925	0.617
Mecistops cataphractus–Turnersuchus hingleyae	-6.348551171	0.142
TAXA 1 – TAXA 2	**Coracoid Ct1**	**p-value**
Neosteneosaurus edwardsi–Mecistops cataphractus	-1.226649234	0.157
Mecistops cataphractus–Hyposaurus natator	-3.769987469	0.151
Hyposaurus natator–Tyrannoneustes lythrodectikos	-2.214239155	0.455
Mycterosuchus nasutus–Neosteneosaurus edwardsi	-0.533893141	0.287
Neosteneosaurus edwardsi–Tyrannoneustes lythrodectikos	-0.064509639	0.14
Tyrannoneustes lythrodectikos–Thalattosuchus superciliosus	-0.37416012	0.792
TAXA 1 – TAXA 2	**Humerus Ct1**	**p-value**
Thalattosuchus superciliosus–Congosaurus bequaerti	-0.413213837	0.077
Hyposaurus natator–Mecistops cataphractus	-4.616547544	0.434
Mecistops cataphractus–Neosteneosaurus edwardsi	-0.574913049	0.107
Hyposaurus natator–Mycterosuchus nasutus	-0.628090812	0.148
Thalattosuchus superciliosus–Tyrannoneustes lythrodectikos	0.27793589	**0.008***
Thalattosuchus superciliosus–Charitomenosuchus leedsi	0.052710017	0.212
Mycterosuchus nasutus–Charitomenosuchus leedsi	-0.275717374	0.914
TAXA 1 – TAXA 2	**Ilium Ct1**	**p-value**
Hyposaurus natator–Mecistops cataphractus	-4.252055871	0.263
Pelagosaurus typus–Mecistops cataphractus	-2.476894754	0.206
Geosaurus giganteus–Hyposaurus natator	-0.546263875	0.075
Neosteneosaurus edwardsi –Mecistops cataphractus	-1.681521311	0.525
Tyrannoneustes lythrodectikos–'Metriorhynchus' brachyrhynchus	-1.407764963	0.952
Tyrannoneustes lythrodectikos–Suchodus durobrivensis	-2.130806776	0.682
Geosaurus giganteus–Cricosaurus araucanensis	-1.568441299	0.58
Pelagosaurus typus–Lemmysuchus obtusidens	-1.643484815	0.927
TAXA 1 – TAXA 2	**Ischium Ct1**	**p-value**
Acherontisuchus guajiraensis–Mecistops cataphractus	-11.35644855	0.572
Thalattosuchus superciliosus–Mecistops cataphractus	-2.360364905	0.789
Lemmysuchus obtusidens–Hyposaurus natator	-1.513413671	0.614
'Metriorhynchus' brachyrhynchus–Torvoneustes carpenteri	-1.423059663	0.586
Charitomenosuchus leedsi–Thalattosuchus superciliosus	-0.139834934	0.731
Neosteneosaurus edwardsi–'Metriorhynchus' brachyrhynchus	-0.337013741	0.887
TAXA 1 – TAXA 2	**Pubis Ct1**	**p-value**
Hyposaurus natator–Pelagosaurus typus	-2.329095035	0.276
Pelagosaurus typus–Mecistops cataphractus	-3.086463592	0.36
Macrospondylus bollensis–Hyposaurus natator	-1.911898822	0.15
Neosteneosaurus edwardsi–Thalattosuchus superciliosus	0.227639595	**0.015***
Macrospondylus bollensis–Pelagosaurus typus	-0.323286053	0.886
Suchodus durobrivensis–Thalattosuchus superciliosus	-0.533485628	0.971
TAXA 1 – TAXA 2	**Femur Ct1**	**p-value**
Mecistops cataphractus–Hyposaurus natator	-3.716742338	0.111
Neosteneosaurus edwardsi–Congosaurus bequaerti	-2.81014971	0.94
Dakosaurus maximus–Mecistops cataphractus	-1.172029451	0.32
Torvoneustes carpenteri–Suchodus durobrivensis	-6.192386098	0.969
Tyrannoneustes lythrodectikos–Neosteneosaurus edwardsi	-0.239081077	0.881
Charitomenosuchus leedsi–'Metriorhynchus' brachyrhynchus	-0.195647626	0.681

TABLE S 5. Pairs of crocodylomorph taxa employed in the Stayton distance-based convergence tests (Ct metrics). 0.05^{*}= significant (α=0.05).

5. LANDMARKS

Bone type	Landmark	Description
Scapula	1	Anterordorsal edge of scapular blade
	2	Anteroventral edge of anterior surface
	3	Anterior edge of scapulocoracoid synchondrosis
	4	Posterior edge of scapulocoracoid synchondrosis at its mid-junction with glenoid process
	5	Posterolateral edge of glenoid process
	6	Posterodorsal edge of scapular blade
Coracoid	1	Anterior edge of coracoid head
	2	Anterior edge of coracoid blade
	3	Posterior edge of coracoid blade
	4	Posterior corner between glenoid process and scapulocoracoid synchondrosis
	5	Maximum curvature of glenoid lip posteriorly
	6	Maximum curvature of ventral edge of glenoid lip
	7	Maximum curvature of anterior edge of glenoid lip
	8	Anterior corner between glenoid process and scapulocoracoid synchondrosis
	9	Anteriormost edge of scapulocoracoid synchondrosis
Humerus	1	Anteriormost tip of anterior capitular tuberosity
	2	Tip of deltopectoral crest
	3	Distal tip/maximum curvature of anterior capitulum
	4	Distal tip/maximum curvature of posterior capitulum
	5	Posteriormost tip of posterior capitular tuberosity
	6	Maximum curvature of dorsal capitular tuberosity lip
	7	Ventralmost tip of anterior capitulum
	8	Ventralmost tip of posterior capitulum

TABLE S 6. Type II Landmarks list.

Bone type	Landmark	Description
Ilium	1	Tip of preacetabular process
	2	Ventral base of preacetabular process
	3	Ventral extremity of supraacetabular crest
	4	Dorsal edge of pubic peduncle lip along anterior side of ilium
	5	Maximum curvature of ventral edge of pubic peduncle
	6	Tip of re-entrant angle of the pubic peduncle lip laterally
	7	Edge of the pubic peduncle bordering the acetabular perforation ventrally
	8	Edge of the ischial peduncle bordering the acetabular perforation ventrally
	9	Posterior extremity of the ischial peduncle lip
	10	Posteroventral edge of the ilium
	11	Maximum curvature of concave margin between ischial peduncle and postacetabular process
	12	Tip of postacetabular process
	13	Dorsal base of preacetabular process
	14	Most laterally protruding point of supraacetabular crest
Ischium	1	Ventral edge of anterior peduncle lip
	2	Ventral base of peduncle bridge
	3	Tip of anterior process
	4	Tip of posterior process
	5	Posterior edge of posterior peduncle at junction with suture area
	6	Anterior edge of posterior peduncle at mid width
	7	Maximum concavity of acetabular perforation
	8	Dorsal edge of anterior peduncle lip
	9	Anterior tip of anterior peduncle
	10	Laterodorsal edge of anterior peduncle lip
	11	Maximum curvature of posterior peduncle anteriorly
Pubis	1	Medial edge of peduncle
	2	Medial constriction of the shaft
	3	Dorsal tip of pubic diaphysis
	4	Ventral tip of pubic diaphysis
	5	Lateral tip of distal blade
	6	Lateral constriction of the shaft
	7	Lateral edge of peduncle
	8	Maximum thickness of pubis ventrally
Femur	1	Anterior tip of femoral head lip
	2	Posterior tip of femoral head lip
	3	Dorsal tip of posterior capitulum
	4	Ventral tip of posterior capitulum
	5	Dorsal tip of anterior capitulum
	6	Ventral tip of anterior capitulum
	7	Maximum edge of femoral head lip laterally
	8	Tip of fourth trochanter

TABLE S 7. Type II Landmarks list.

Bone type	Curve	Points	Density	Description
Scapula	1	5	33	Anterior surface of scapula, joining Single Point 1 to 2
	2	3	7	Anterior surface of scapula, joining Single Point 2 to 3
	3	3	17	Midline of scapulocoracoid synchondrosis, joining Single Point 3 to 4
	4	3	13	Midline of glenoid process, joining Single Point 4 to 5
	5	5	33	Posterior surface of scapula, joining Single Point 5 to 6
	6	4	28	Dorsal surface of scapular blade, joining Single Point 6 to 1
	7	8	41	Scapulocoracoid synchondrosis outline, going laterally from Single Point 4
	8	6	31	Glenoid outline, going laterally from Single Point 5
Coracoid	1	5	33	Anterior surface of coracoid, joining Single Point 1 to 2
	2	4	25	Distal surface of coracoid blade, joining Single Point 2 to 3
	3	5	33	Posterior surface of coracoid until base of glenoid, joining Single Point 3 to 4
	4	4	22	Midline of scapulocoracoid synchondrosis, joining Single Point 4 to 9
	5	3	19	Anterior surface of coracoid, joining Single Point 9 to 1
	6	6	31	Glenoid outline, going posteriorly from Single Point 4
	7	7	36	Scapulocoracoid synchondrosis outline, going anteriorly from Single Point 8
Humerus	1	4	16	ACT lip to tip of deltopectoral crest, joining Single Point 1 to 2
	2	7	31	Deltopectoral crest to max curvature of anterior capitulum, joining Single Point 2 to 3
	3	3	11	Max curvature of anterior capitulum to posterior capitulum, joining Single Point 3 to 4
	4	7	43	Max curvature of posterior capitulum to PCT lip, joining Single Point 4 to 5
	5	4	16	Maximal curvature of humeral head, joining Single Point 5 to 1
	6	7	25	Lip of distal condyles, going anteriorly from Single Point 7 to point 8
	7	4	13	Ventral lip of trochlea between distal condyles, joining Single Point 8 to 7
	8	8	33	Outline of humeral head lip, going anteriorly from Single Point 6
Ilium	1	3	19	Anterior margin of ilium, joining Single Point 1 to 4
	2	5	21	Ventral margin of pubic peduncle, joining Single Point 4 to 7
	3	3	11	Acetabular perforation, joining Single Point 7 to 8
	4	5	21	Ventral margin of ischial peduncle, joining Single Point 8 to 9
	5	6	26	Posterior margin of ilium, joining Single Point 10 to 12
	6	6	26	Dorsal margin of ilium, joining Single Point 12 to 1
	7	15	71	Dorsal outline of peduncles, joining Single Point 4 to 9
	8	4	16	Supraacetabular crest, joining Single Point 3 to 14
Ischium	1	5	25	Anterior concavity of ischium, joining Single Point 1 to 3
	2	5	25	Distal blade of ischium, joining Single Point 3 to 4
	3	6	26	Posterior surface of ischium, joining Single Point 4 to 5
	4	3	11	Midline of posterior peduncle, joining Single Point 5 to 6
	5	3	11	Midline of acetabular perforation, joining Single Point 6 to 8
	6	3	11	Midline of anterior peduncle, joining Single Point 8 to 1
	7	8	33	Outline of acetabulum facet of posterior peduncle, going posteriorly from Single Point 7
	8	8	33	Outline of anterior peduncle lip, going medially from Single point 11
Pubis	1	5	25	Medial surface of pubis, joining Single Point 1 to 3
	2	3	13	Pubic diaphysis surface, joining Single Point 3 to 4
	3	4	19	Distal blade surface, joining Single Point 4 to 5
	4	6	31	Lateral surface of pubis, joining Single Point 5 to 7
	5	3	13	Maximum curvature of peduncle, joining Single Point 7 to 1
	6	6	19	Outline of peduncle lip, going laterally from Single Point 1
Femur	1	5	37	Anterior surface from femoral head to tip of anterior capitulum, joining Single Point 1 to 3
	2	5	37	Posterior surface from tip of anterior capitulum to femoral head, joining Single Point 4 to 2
	3	8	33	Outline of distal condyles lip, going posteriorly from Single Point 3
	4	8	33	Outline of femoral head lip, going posteriorly from Single Point 1

TABLE S 8. Semi-landmarks list. ACT: anterior capitular tuberosity. PCT: posterior capitular tuberosity.

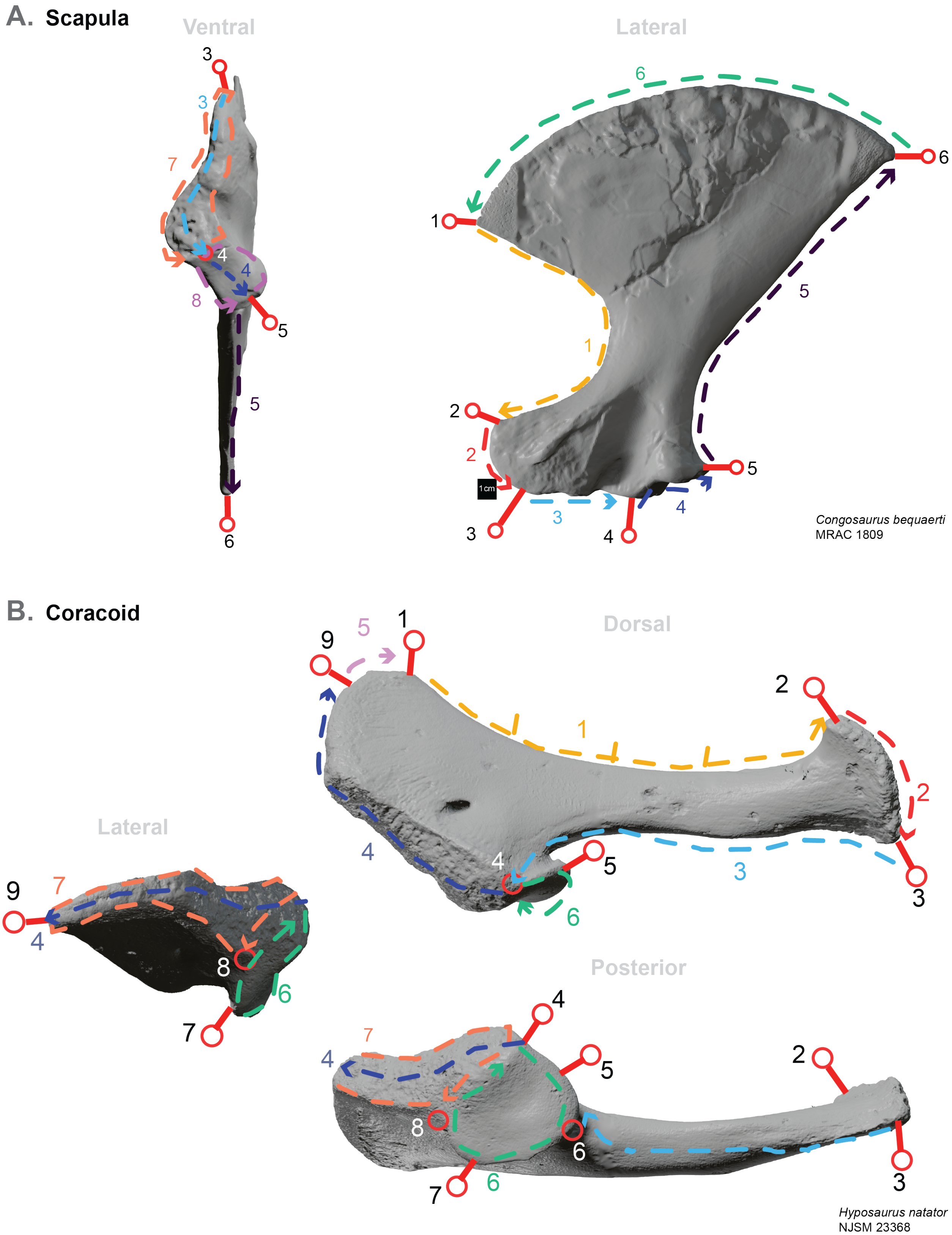

FIGURE S 19. Positioning of Type II Landmarks and semi-landmarks. Type II Landmarks are represented by a circle and semi-landmarks are represented by coloured dashed lines. **A.** Scapula ; **B.** Coracoid.

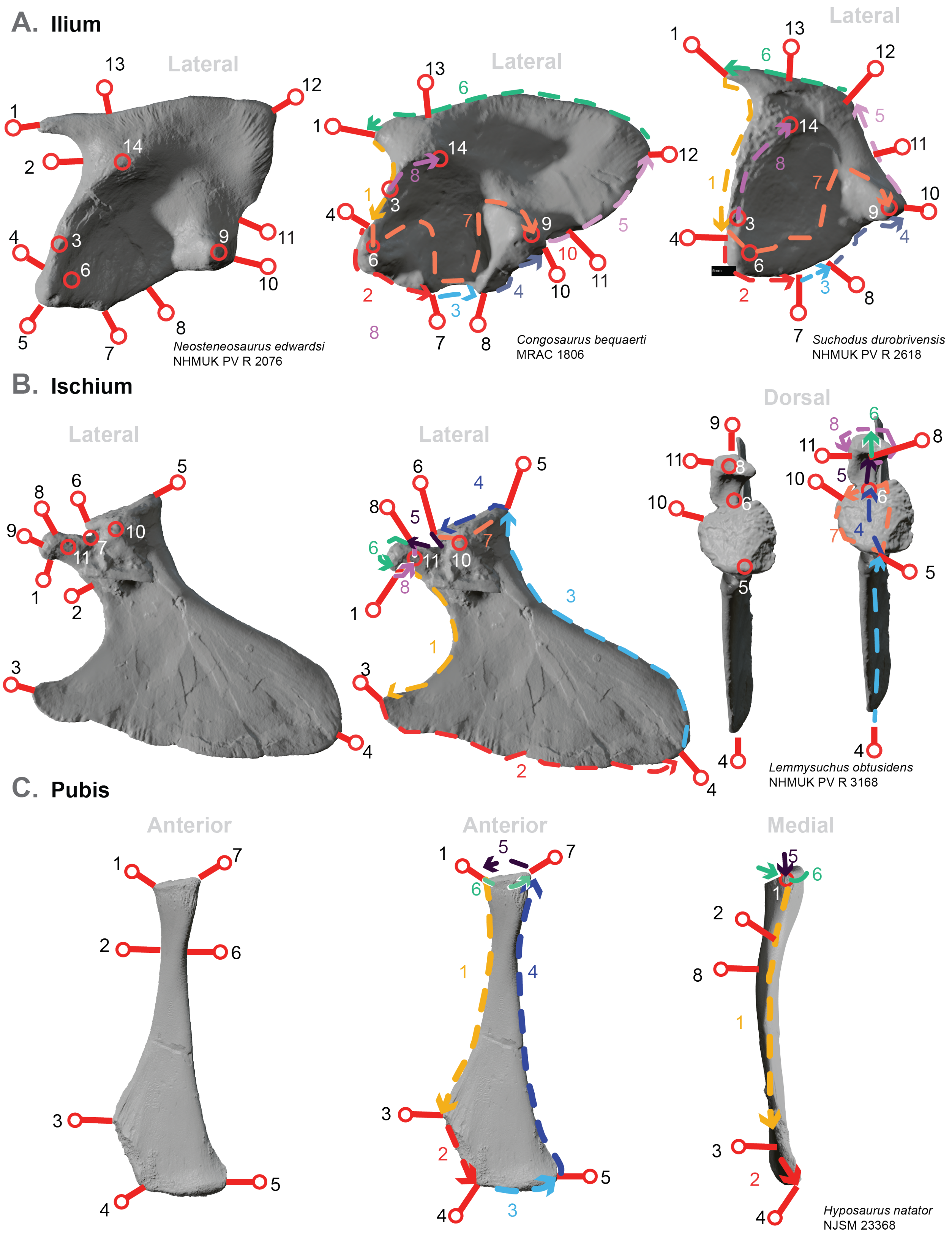

FIGURE S 20. Positioning of Type II Landmarks and semi-landmarks. Type II Landmarks are represented by a circle and semi-landmarks are represented by coloured dashed lines. **A.** Ilium ; **B.** Ischium ; **C.** Pubis.

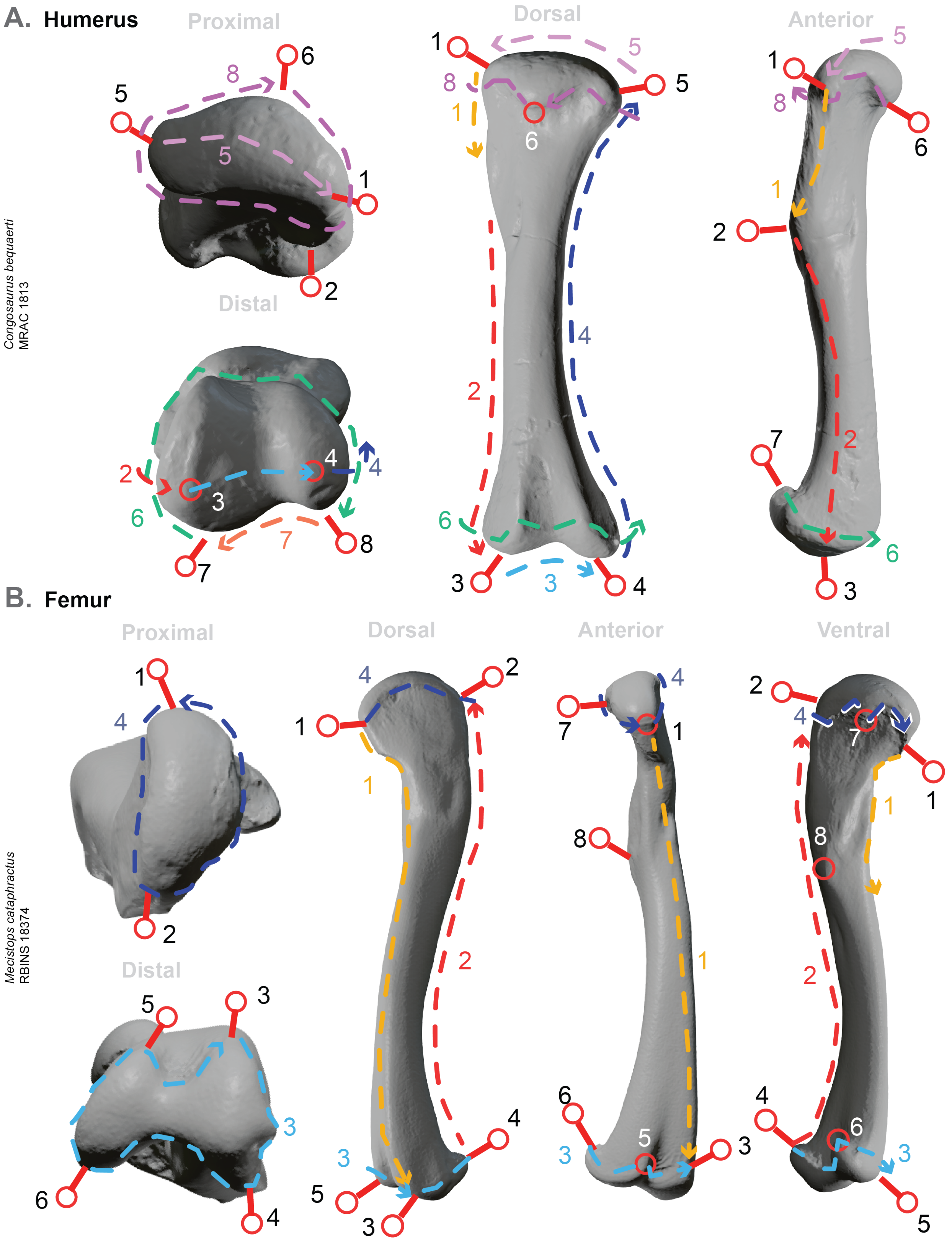

FIGURE S 21. Positioning of Type II Landmarks and semi-landmarks. Type II Landmarks are represented by a circle and semi-landmarks are represented by coloured dashed lines. **A.** Humerus ; **B.** Femur.

6. Isolated bone morphospaces

On the scapulae we placed 6 type-II landmarks (Bookstein 1997) using the software Stratovan Checkpoint (version 2020.10.13.0859). We added a total of 8 curves comprising a total of 187 sliding semi-landmarks: 31 have been allocated to mark the shape of the glenoid process, 41 along the rim of the scapulocoracoid synchondrosis, and 115 have been placed around the outline of the scapula.

On the coracoids we placed 9 type-II landmarks (Bookstein 1997) using the software Stratovan Checkpoint (version 2020.10.13.0859). We added a total of 7 curves comprising a total of 185 sliding semi-landmarks: 31 have been allocated to mark the shape of the glenoid process, 36 along the rim of the scapulocoracoid synchondrosis, and 118 have been placed around the outline of the coracoid.

On the humeri we placed 8 type-II landmarks (Bookstein 1997) using the software Stratovan Checkpoint (version 2020.10.13.0859). We added a total of 8 curves comprising a total of 172 sliding semi-landmarks: 33 have been allocated to mark the shape of the proximal head, 38 along the rim of the distal condyles, and 101 have been placed around the outline of the humerus.

On the ilia, we placed 14 type-II landmarks (Bookstein 1997) using the software Stratovan Checkpoint (version 2020.10.13.0859). We added a total of 8 curves comprising a total of 195 sliding semi-landmarks: 71 have been allocated to mark the shape of both pubic and ischial peduncles, 129 have been placed around the outline of the ilium.

On the ischia we placed 11 type-II landmarks (Bookstein 1997) using the software Stratovan Checkpoint (version 2020.10.13.0859). We added a total of 8 curves comprising a total of 159 sliding semi-landmarks: 66 have been allocated to mark the shape of both anterior and posterior peduncles, 93 have been placed around the outline of the ischium.

On the pubes we placed 8 type-II landmarks (Bookstein 1997) using the software Stratovan Checkpoint (version 2020.10.13.0859). We added a total of 5 curves comprising a total of 169 sliding semi-landmarks: 37 have been allocated to mark the shape of the peduncle, 132 have been placed around the outline of the pubis.

On the femora we placed 8 type-II landmarks (Bookstein 1997) using the software Stratovan Checkpoint (version 2020.10.13.0859). We added a total of 4 curves comprising a total of 132 sliding semi-landmarks: 33 have been allocated to mark the shape of the proximal head, 33 along the rim of the distal condyles, and 74 have been placed around the outline of the femur.

In every single bone morphospace, the first axis of the PCA accounts for the majority of the relative eigenvalue: 65.52% for the ilium, 58.59% for the ischium, 30% for the pubis, 57.17% for the femur, 64.83% for the coracoid, 79.19% for the scapula and 61.05% for the humerus. The second axis of the PCA represents only a fraction of the relative eigenvalue in most cases: 10.45% for the ischium, 8.93% for the ilium, 12.77% for the femur, 15.4% for the coracoid, 9.55% for the scapula, and 17.8% for the humerus. For the pubis, the second axis of the PCA is proportionally greater and reaches 23.33%.

On most single bone analysis (see Figures 22 and 23), Thalattosuchia, Dyrosauridea and Crocodylia occupy clearly distinct areas of the morphospaces, with the femur and pubis as only exceptions. Within Thalattosuchia, the subclades Teleosauroidea and Metriorhynchoidea appear to cover specific regions of the morphospaces, often markedly distinct from one another resulting in a large morphospace occupation for Thalattosuchia. The phylogenetic influence seems strong along both axes of each PCA for the

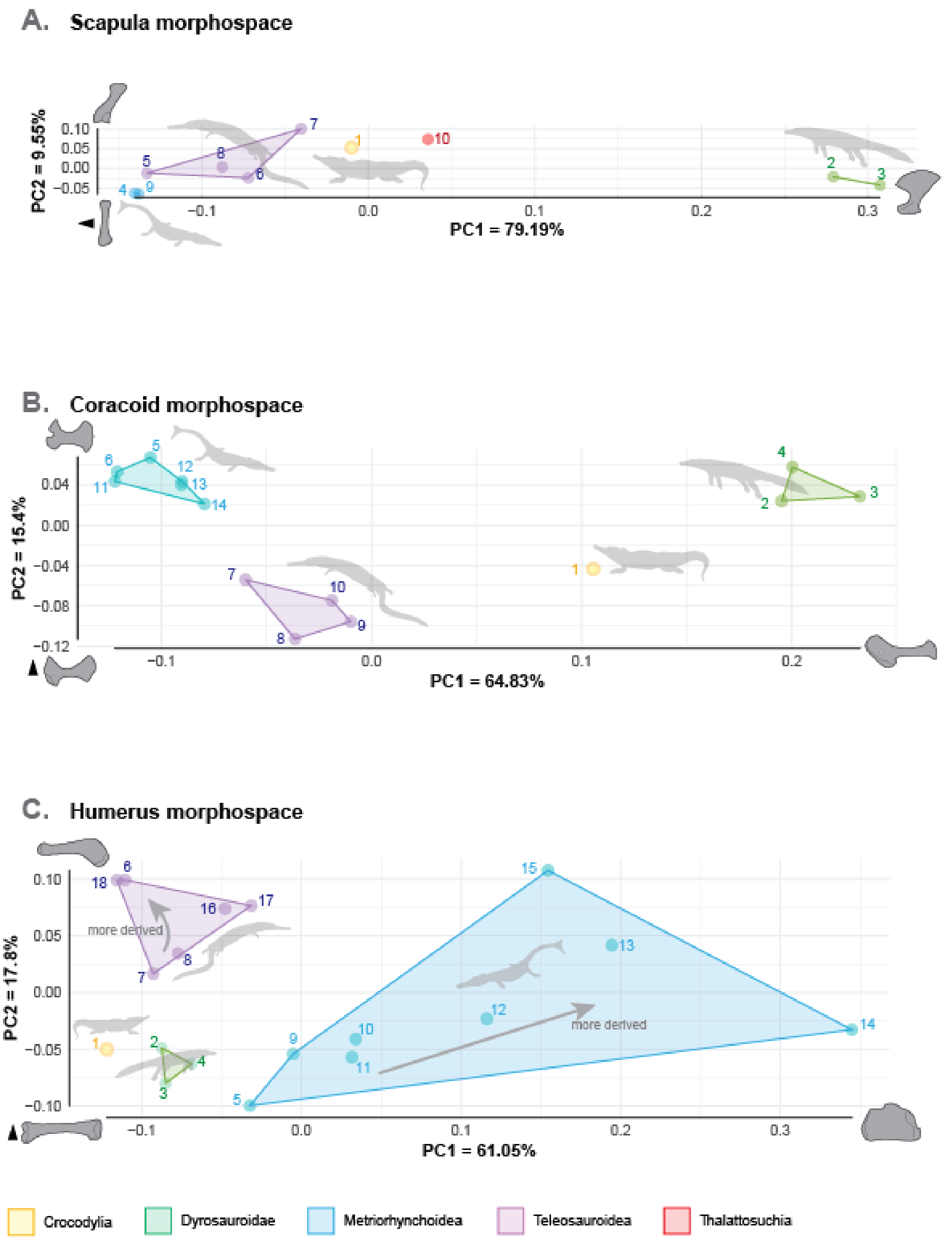

FIGURE S 22. Morphospaces representing dissimilarity between Dyrosauridea, Crocodylia, Metriorhynchoidea (Thalattosuchia) and Teleosauroidea (Thalattosuchia) using the first two PCA axes. **A.** morphospace based on the scapula landmarks. *1: Mecistops cataphractus* RBINS 18374; *2: Congosaurus bequaerti* MRAC 1809; *3: Hyposaurus natator* NJSM 23368; *4: Thalattosuchus superciliosus* PMU 35988; *5: Charitomenosuchus leedsi* NHMUK PV R 3806; *6: Neosteneosaurus edwardsi* NHMUK PV R 3701; *7: Mycterosuchus nasutus* NMH PV R 2617; *8: Lemmysuchus obtusidens* NHMUK PV R 3168; *9: 'Metriorhynchus' superciliosus* GLAHM V1146; *10: Turnersuchus hingleyae* LYMPH 2021/45. **B.** morphospace based on the coracoid landmarks. *1: Mecistops cataphractus* RBINS 18374; *2: Hyposaurus natator* YPM VP.000985; *3: Hyposaurus natator* NJSM 23368; *4: Congosaurus bequaerti* MRAC 1811: *5: Thalattosuchus superciliosus* PMU 35988; *6: Thalattosuchus superciliosus* NHMUK PV R 1530; *7: 'Neosteneosaurus edwardsi'* NHMUK PV R 3169; *8: Charitomenosuchus leedsi* NHMUK PV R 3806; *9: Mycterosuchus nasutus* NHMUK PV R 2617; *10: Neosteneosaurus edwardsi* NHMUK PV R 3701; *11:Thalattosuchus superciliosus* GLAHM V1143; *12: 'Thalattosuchus' superciliosus* GLAHM V1146; *13: 'Thalattosuchus' superciliosus* GLAHM V1005; *14: Tyrannoneustes lythrodectikos* GLAHM V1145. **C.** morphospace based on the humerus landmarks. *1: Mecistops cataphractus* RBINS 18374; *2: Hyposaurus natator* NJSM 23368; *3: Hyposaurus natator* YPM VP.000985; *4: Congosaurus bequaerti* MRAC 1813; *5: Thalattosuchus superciliosus* NHMUK PV R 2032; *6: Neosteneosaurus edwardsi* NHMUK PV R 3701; *7: Charitomenosuchus leedsi* NHMUK PV R 3806; *8: Mycterosuchus nasutus* NHMUK PV R 2617; *9: 'Metriorhynchus' superciliosus* GLAHM V1016; *10: Tyrannoneustes lythrodectikos* GLAHM V1145; *11: Thalattosuchus superciliosus* GLAHM V1143; *12: 'Thalattosuchus' superciliosus* GLAHM V1146; *13: Torvoneustes carpenteri* BRSMG Cd7203; *14: Geosaurus lapparenti* UJF–ID.11846m; *15: Dakosaurus maximus* SMNS 8203; *16: Proexochokefalos* cf. *bouchardi* SCR010-374; *17: Sericodon jugleri* SCR010-312; *18: Lemmysuchus obtusidens* NHMUK PV R 3168. Crocodylia vector by Smokeybjb (vectorized by T. Michael Keesey); Dyrosauridea vector Nobu Tamura (vectorized by Zimices) Thalattosuchia by Gareth Monger. Autopodium from *Dyrosaurus maghribiensis* OCP DEK-GE 252 resized to fit *Congosaurus bequaerti* MRAC 1813 (based on humerus); autopodium from *Platysuchus multiscrobiculatus* SMNS 9930 resized to fit *Charitomenosuchus leedsi* NHMUK PV R 3806 (based on humerus); autopodium from *Mecistops cataphractus* RBINS 11839 to illustrate Crocodylia. Crocodylomorphs silhouettes: Metriorhynchoidea & Teleosauroidea (c) Gareth Monger – Licence CC BY 3.0; Dyrosauridae (c) Nobu Tamura, vectorized by Zimices – Licence CC BY-SA 3.0; Crocodylia original picture (c) Thesupermart – License CC BY-SA 3.0.Arrow points anteriorly. Target indicates anterior view.

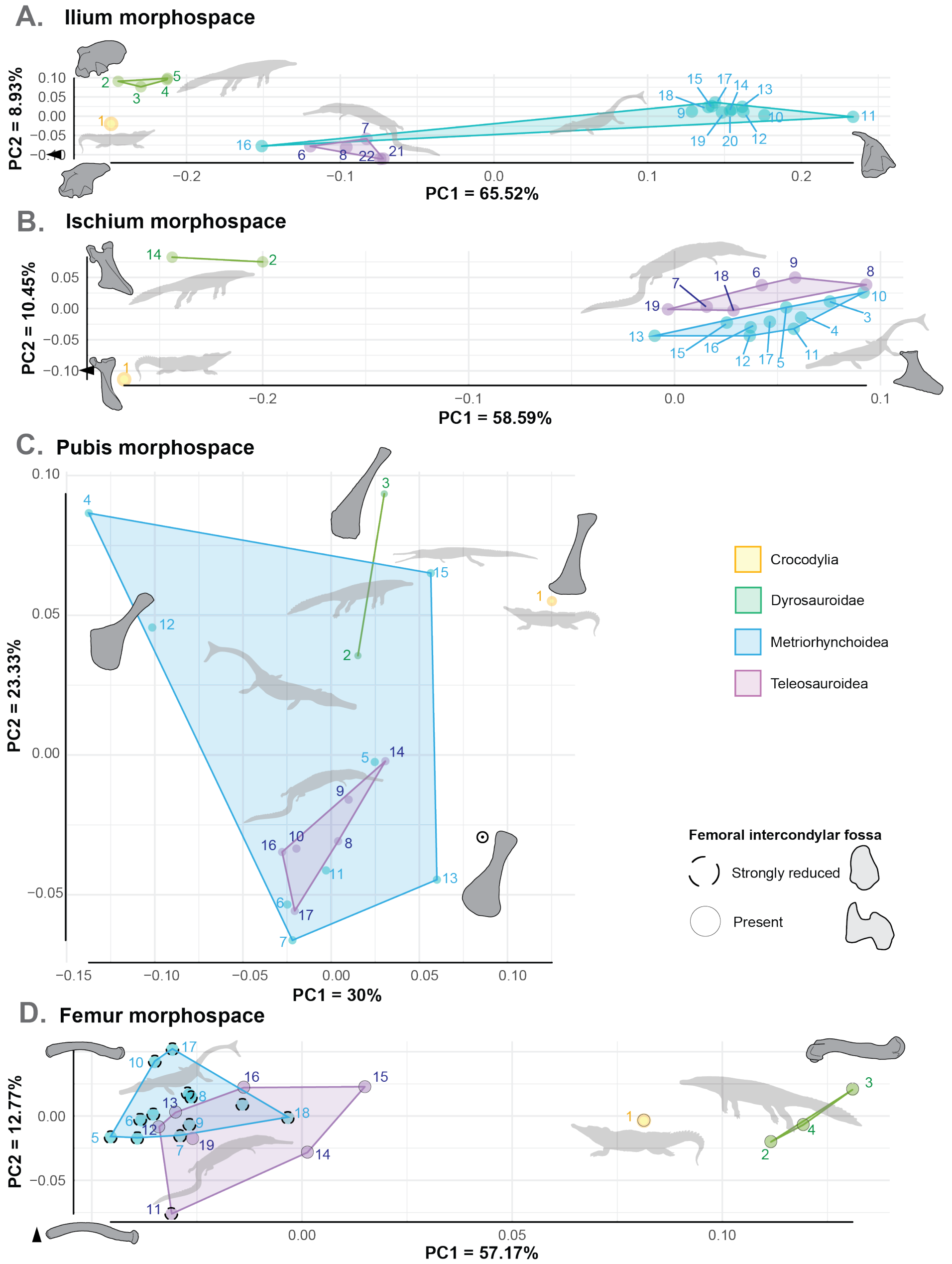

FIGURE S 23. Morphospaces representing dissimilarity between Dyrosauridea, Crocodylia, Metriorhynchoidea (Thalattosuchia) and Teleosauroidea (Thalattosuchia) using the first two PCA axes. **A.** morphospace based on the ilium landmarks. *1: Mecistops cataphractus*; *2: Hyposaurus natator* NJSM 23368; *3: Hyposaurus natator* YPM VP.000753; *4: Acherontisuchus guajiraensis* UF/IGM 38; *5: Congosaurus bequaerti* MRAC 1806; *6: Lemmysuchus obtusidens* NHMUK PV R 3168; *7: Neosteneosaurus edwardsi* NHMUK PV R 2076; *8: Charitomenosuchus leedsi* NHMUK PV R 3806; *9: Thalattosuchus superciliosus* NHMUK PV R 1530; *10: Cricosaurus araucanensis* MLP 72-IV-7-1; *11: 'Metriorhynchus' brachyrhynchus* NHMUK PV R 4763; *12: Thalattosuchus superciliosus* NHMUK PV R 2054; *13: 'Metriorhynchus' brachyrhynchus* NHMUK PV R 3804; *14: Suchodus durobrivensis* NHMUK PV R 2618; *15: Geosaurus giganteus* NHMUK PV R 1230; *16: Pelagosaurus typus* BRLSI M.1417; *17: Tyrannoneustes lythrodectikos* GLAHM V972; *18: Thalattosuchus superciliosus* GLAHM V1005; *19: Thalattosuchus superciliosus* GLAHM V1146; *20: Tyrannoneustes lythrodectikos* GLAHM V1145; *21: Proexochokefalos cf. bouchardi* SCR010-374; *22: Sericodon jugleri* SCR010-312. **B.** morphospace based on the ischium landmarks. *1: Mecistops cataphractus* RBINS 18374; *2: Hyposaurus natator* NJSM 23368; *3: Thalattosuchus superciliosus* NHMUK PV R 1530; *4: 'Metriorhynchus' brachyrhynchus* NHMUK PV R 4763; *5: Thalattosuchus superciliosus* NHMUK PV R 2054; *6: Neosteneosaurus edwardsi* NHMUK PV R 3701; *7: Charitomenosuchus leedsi* NHMUK PV R 3806; *8: Neosteneosaurus edwardsi* NHMUK PV R 2865; *9: Lemmysuchus obtusidens* NHMUK PV R 3168; *10: 'Metriorhynchus' brachyrhynchus* NHMUK PV R 3804; *11:Torvoneustes carpenteri* BRSMG Cd7203; *12: Pelagosaurus typus* BRLSI M.1410; *13: 'Thalattosuchus' superciliosus* GLAHM V950; *14; Acherontisuchus guajiraensis* UF/IGM 38; *15: 'Metriorhynchus' superciliosus* GLAHM V960 [1]; *16: Thalattosuchus superciliosus* GLAHM V1005; *17: 'Metriorhynchus' superciliosus* GLAHM V960 [2]; *18: Sericodon jugleri* SCR010-312; *19: Proexochokefalos cf. bouchardi* SCR010-374. **C.** morphospace based on the pubis landmarks. *1: Mecistops cataphractus* RBINS 18374; *2: Hyposaurus natator* NJSM 23368; *3: Hyposaurus natator* YPM VP.000753; *4: 'Metriorhynchus' brachyrhynchus* NHMUK PV R 3804; *5: Thalattosuchus superciliosus* NHMUK PV R 2618; *7: Thalattosuchus superciliosus* NHMUK PV R 1530; *8: Neosteneosaurus edwardsi* NHMUK PV R 2076; *9: Neosteneosaurus edwardsi* NHMUK PV R 3701; *10: Charitomenosuchus leedsi* NHMUK PV R 3806; *11:'Thalattosuchus' superciliosus* GLAHM V960; *12:'Thalattosuchus' superciliosus* GLAHM V1005; *13: Geosaurus giganteus* NHMUK PV R 1230; *14: Macrospondylus bollensis* NHMUK PV R 5703; *15: Pelagosaurus typus* BRLSI M.1420; *16: Machimosaurus hugii* SMNS 81608; *17: Lemmysuchus obtusidens* NHMUK PV R 3168. **D.** morphospace based on the femur landmarks. *1: Mecistops cataphractus* RBINS 18374; *2: Hyposaurus natator* YPM VP.000753; *3: Congosaurus bequaerti* MRAC 1817; *4: Hyposaurus natator* NJSM 233368; *5: Thalattosuchus superciliosus* NHMUK PV R 1530; *6: Thalattosuchus superciliosus* NHMUK PV R 2054; *7: Thalattosuchus superciliosus* NHMUK PV R 2032; *8: Suchodus durobrivensis* NHMUK PV R 2618; *9: 'Metriorhynchus' brachyrhynchus* NHMUK PV R 4763; *10: 'Metriorhynchus' brachyrhynchus* NHMUK PV R 3804; *11: Machimosaurus hugii* SMNS 81608; *12: Charitomenosuchus leedsi* NHMUK PV R 3806; *13: Neosteneosaurus edwardsi* NHMUK PV R 2865; *14: Lemmysuchus obtusidens* NHMUK PV R 3168; *15: Neosteneosaurus edwardsi* NHMUK PV R 3169; *16: Neosteneosaurus edwardsi* NHMUK PV R 2076; *17:'Thalattosuchus' superciliosus* GLAHM V1005; *18: Dakosaurus maximus* SMNS 8203; *19: Sericodon jugleri* SCR010-312. Crocodylomorphs silhouettes: Metriorhynchoidea & Teleosauroidea (c) Gareth Monger – Licence CC BY 3.0; Dyrosauridae (c) Nobu Tamura, vectorized by Zimices – Licence CC BY-SA 3.0; Crocodylia original picture (c) Thesupermart – License CC BY-SA 3.0; *Pelagosaurus typus* vector (c) Scott Hartman – License CC BY 3.0. Arrow points anteriorly. Target indicates anterior view.

scapula, coracoid, ilium, ischium, and femur (mantel test: scapula r=0.544 & p=0.025; coracoid r=0.852 & p=0.001; ilium r= 0.6589 & p=0.001; ischium r=0.9178 & p=0.001; femur r=0.8546 & p=0.001). However, the mantel test does not recover any significant correlation between phylogenetic distance and phenotypic distance for the humerus (r=0.1947 & p=0.133) and pubis (r=0.322 & p=0.043). ANOVA test results (p-value) indicate that Crocodylia, Dyrosauridea, Metriorhynchoidea and Teleosauroidea are significantly dissimilar in each case: ilium p-value is 0.001, ischium p-value is 0.001, pubis p-value is 0.01, femur p-value is 0.001, scapula p-value is 0.001, coracoid p-value is 0.001, humerus p-value is 0.003.

Thalattosuchus superciliosus is responsible is scattered in the ilium and pubis analyses. The strong intraspecific variance of this taxa suggests the presence of at least two morphotypes. In parallel, the specimen NHMUK PV R 1530 appears to suffer from hip defect or malformation as both the ilium and pubis display flattened and rugged bone surface. The femur also shows a less clear signal perhaps due to its strong sensitivity to taphonomic induced deformations. Notably, larger thalattosuchian femora were more subject to deformations compared to other limb bones of the same specimen, regardless of the family and osteoporotic state [Hua and De Buffrenil, 1996]. For this reason, we thoroughly defined a landmarking protocol which takes this issue into account. As a result, the metriorhynchoid and teleosauroid femora appear superficially similar but are anatomically different in detail (namely the deletion of the trochlear groove in metriorhynchoids).

7. Combined landmark coordinates

Some taxa possess complete specimens regarding their girdle and hence those were used in their entirety: *Hyposaurus natator* NJSM 23368, *Charitomenosuchus* NHMUK PV R 3806, *Mycterosuchus nasutus* NHMUK PV R 2617 (thoracic only), *Congosaurus bequaerti* MRAC 1806-1809-1813 (thoracic only), and *Mecistops cataphractus* RBINS 18374.

Some taxa only possess incomplete specimens and required the use of different parts to create the combined landmark datasets. We chose the best preserved bones among the specimens for each taxa. *Thalattosuchus superciliosus* coracoid, ilium and ischium are NHMUK PV R 1530, pubis and femur are NHMUK PV R 2054, scapula is PMU 35988 and humerus is NHMUK PV R 2032. *Thalattosuchus superciliosus* GLAHM V1143 shares the scapula of *'Thalattosuchus' superciliosus* GLAHM V1146. *'Metriorhynchus' brachyrhynchus* NHMUK PV R 4763 shares the pubis of NHMUK PV R 3804. *Neosteneosaurus edwardsi* ilium and femur are NHMUK PV R 2076, ischium, pubis, scapula, coracoid and humerus are NHMUK PV R 3701. *Lemmysuchus obtusidens* comprises all girdle elements of NHMUK PV R 3168, except the coracoid which is NHMUK PV R 3169.

On the combined morphospaces, the first axis of the PCA represents the majority of the relative eigenvalue in each graph: 60.19% for the thoracic combined dataset, 58.07% for the pelvic combined dataset, and 56.41% of the relative eigenvalue for the thoracic+pelvic dataset. In comparison, the second axis of the PCA is lesser than the first axis: 17.7% for the thoracic combined dataset, 15.68% for the pelvic combined dataset, and 17.74% of the relative eigenvalue for the thoracic+pelvic dataset. ANOVA test results (p-value) indicate that Crocodylia, Dyrosauridea, Metriorhynchoidea and Teleosauroidea are significantly dissimilar in each case (thoracic dataset $p=0.001$; pelvic dataset $p=0.0015$; thoracic+pelvic dataset $p=0.0385$). In parallel, the mantel test recovers a relatively significant correlation between phylogenetic distance and phenotypic distance for each dataset (thoracic dataset $r=0.6299$ & $p=0.007$; pelvic dataset $r=0.755$ & $p=0.004$; thoracic+pelvic dataset $r=0.845$ & $p=0.036$).

On the total combined (thoracic+pelvic) morphospace (see Figure 31), Dyrosauridea, Crocodylia, Metriorhynchoidea and Teleosauroidea are dissimilar. Following the first axis, Thalattosuchia is strongly isolated whereas Dyrosauridea and Crocodylia appear closer. Teleosauroidea is proportionally closer to Metriorhynchoidea than to Crocodylia or Dyrosauridae on both axes. There is little variance between the taxa of Teleosauroidea compared to the separation between the clades. Still, *Lemmysuchus obtusidens* and *Neosteneosaurus edwardsi* are closer to one another than to *Charitomenosuchus leedsi*, reflecting their closer phylogenetic relationship. Dyrosauridea is isolated on both axes and Thalattosuchia (Metriorhynchoidea and Teleosauroidea) is set between the dyrosaurid and crocodylian configuration. The total combined set shows the strong disparity between Crocodylia, Thalattosuchia and Dyrosauridea but places Crocodylia close to either Dyrosauridea or Teleosauroidea depending on the axis. This reveals the existence of some similarities Crocodylia share with Teleosauroidea (*e.g.* scapula, ilium) and Dyrosauridea (*e.g.* femur, humerus, ilium) without leading to a noticeable convergence.

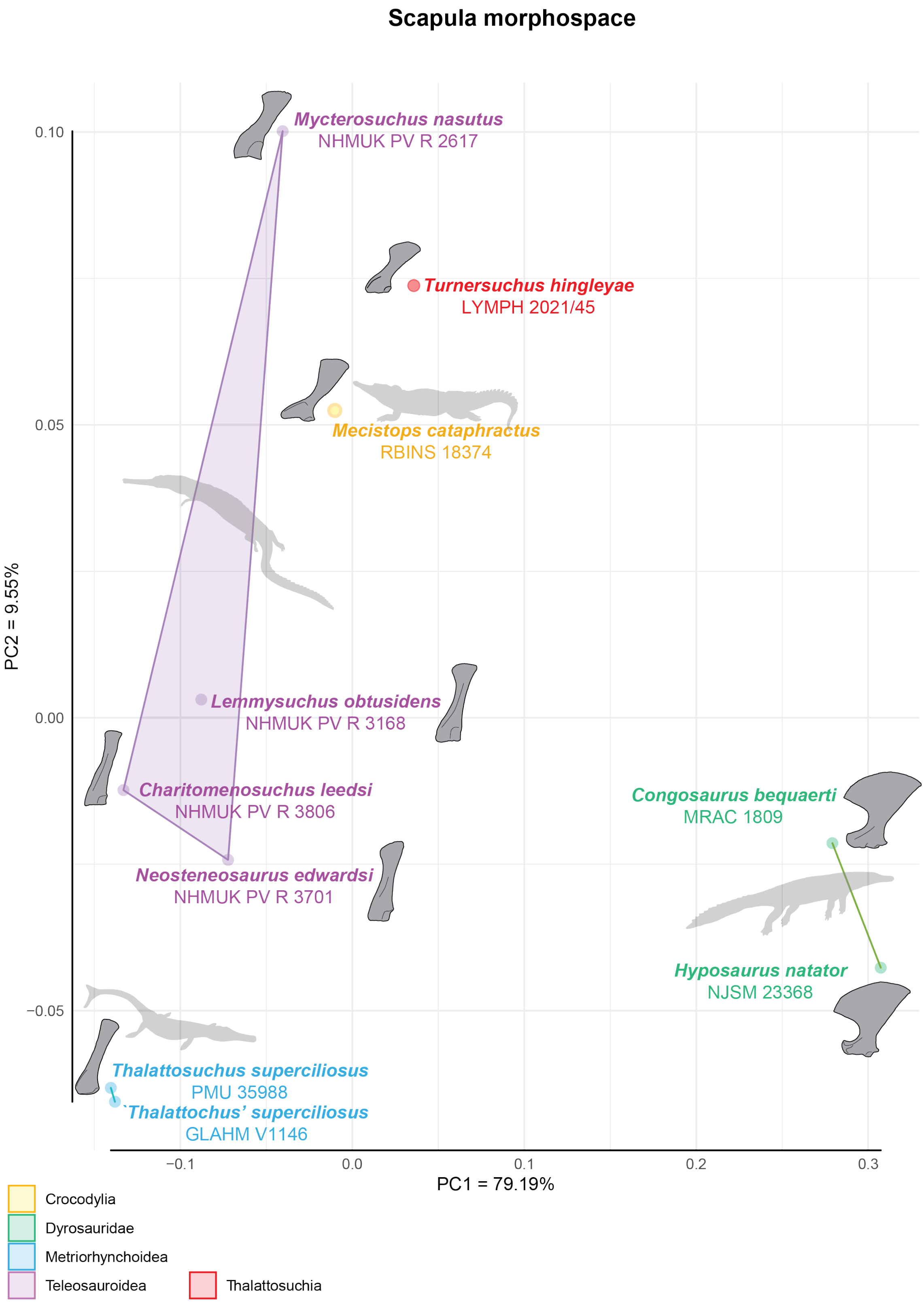

FIGURE S 24. Morphospace representing dissimilarity between the scapulae of Dyrosauridea, Crocodylia, Metriorhynchoidea (Thalattosuchia) and Teleosauroidea (Thalattosuchia) using the first two PCA axes. Crocodylomorphs silhouettes: Metriorhynchoidea & Teleosauroidea (c) Gareth Monger – Licence CC BY 3.0; Dyrosauridae (c) Nobu Tamura, vectorized by Zimices – Licence CC BY-SA 3.0; Crocodylia original picture (c) Thesupermart – License CC BY-SA 3.0.

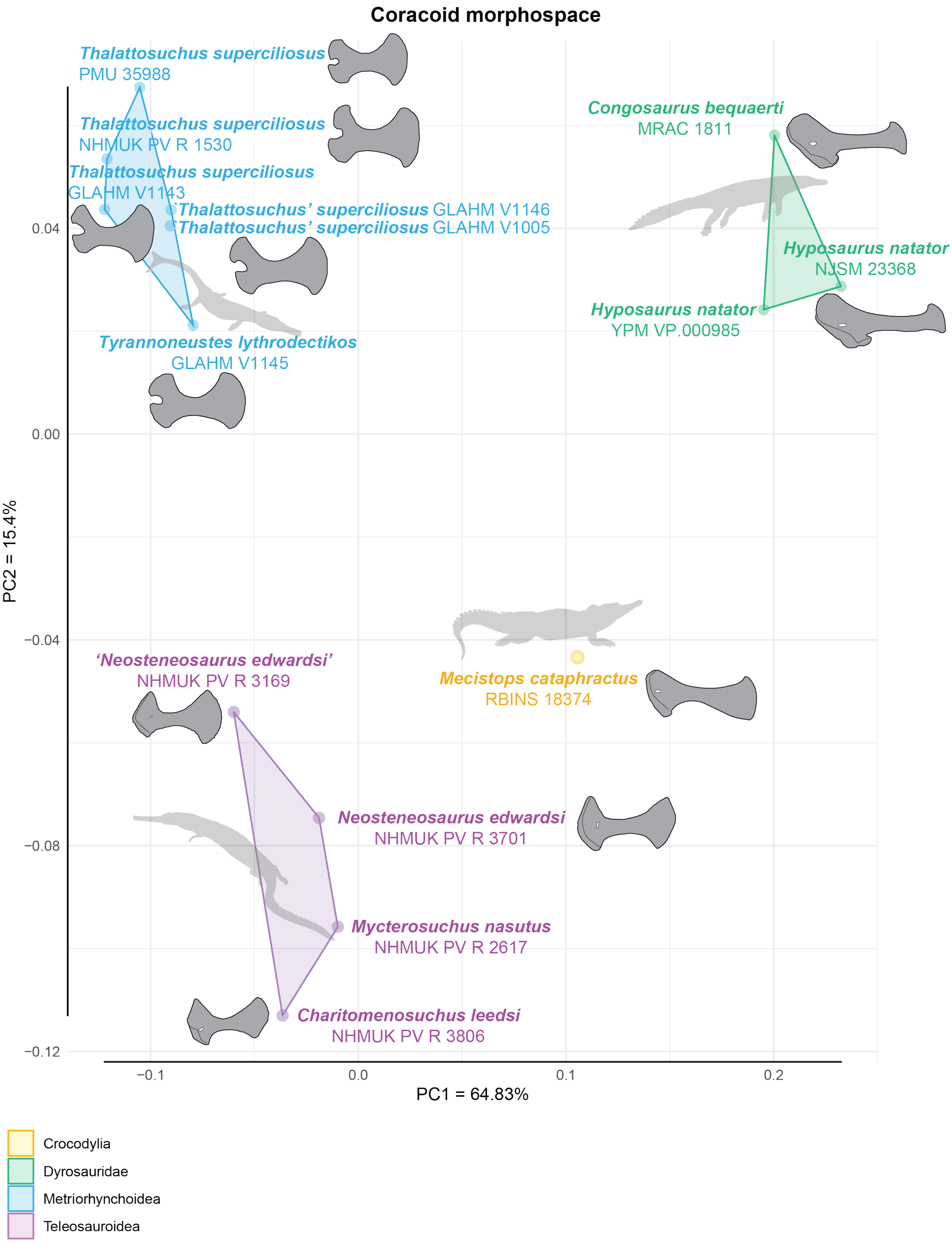

FIGURE S 25. Morphospace representing dissimilarity between the coracoids of Dyrosauridea, Crocodylia, Metriorhynchoidea (Thalattosuchia) and Teleosauroidea (Thalattosuchia) using the first two PCA axes. Crocodylomorphs silhouettes: Metriorhynchoidea & Teleosauroidea (c) Gareth Monger – Licence CC BY 3.0; Dyrosauridae (c) Nobu Tamura, vectorized by Zimices – Licence CC BY-SA 3.0; Crocodylia original picture (c) Thesupermart – License CC BY-SA 3.0.

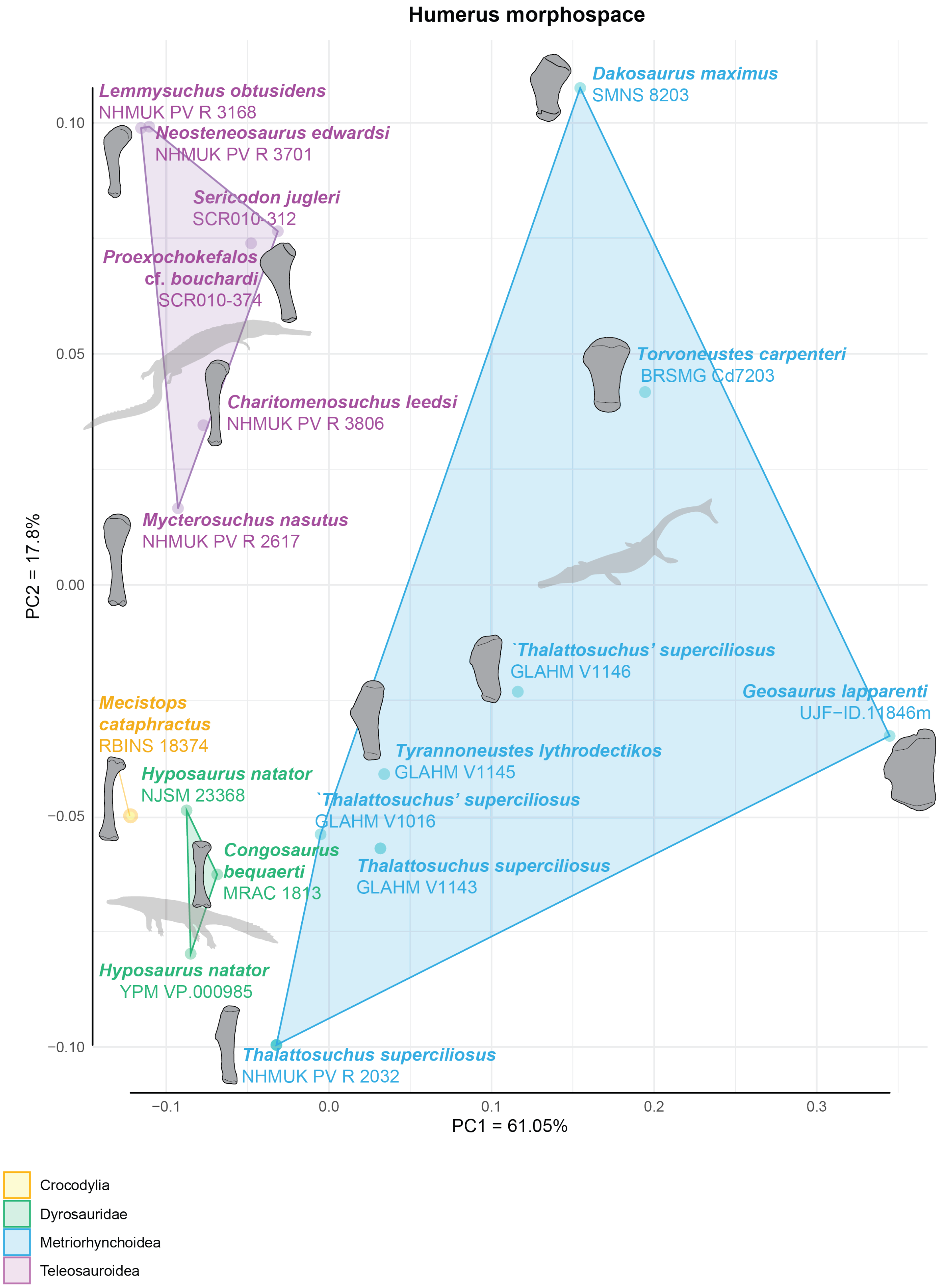

FIGURE S 26. Morphospace representing dissimilarity between the humeri of Dyrosauridea, Crocodylia, Metriorhynchoidea (Thalattosuchia) and Teleosauroidea (Thalattosuchia) using the first two PCA axes. Crocodylomorphs silhouettes: Metriorhynchoidea & Teleosauroidea (c) Gareth Monger – Licence CC BY 3.0; Dyrosauridae (c) Nobu Tamura, vectorized by Zimices – Licence CC BY-SA 3.0; Crocodylia original picture (c) Thesupermart – License CC BY-SA 3.0.

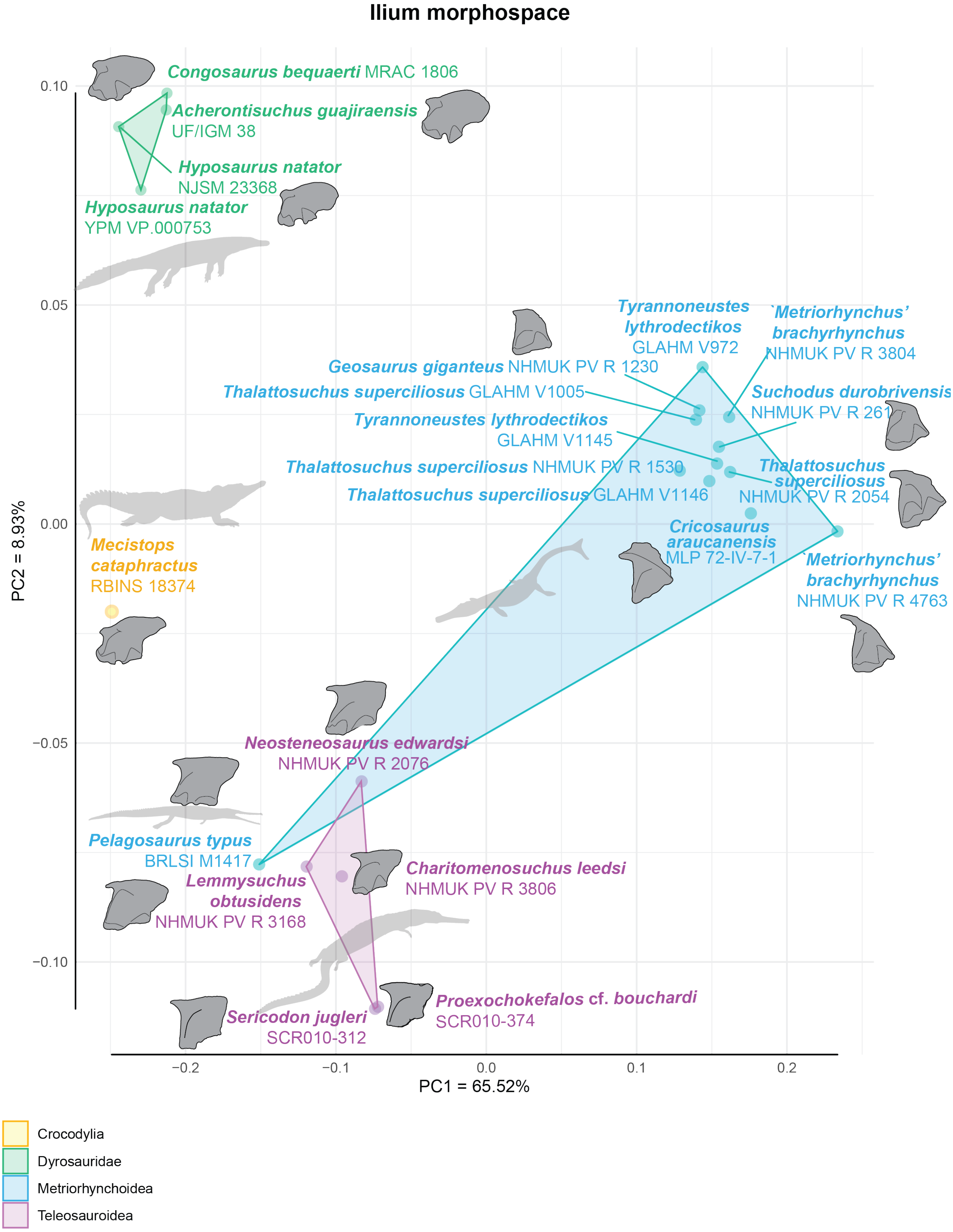

FIGURE S 27. Morphospace representing dissimilarity between the ilia of Dyrosauridea, Crocodylia, Metriorhynchoidea (Thalattosuchia) and Teleosauroidea (Thalattosuchia) using the first two PCA axes. Crocodylomorphs silhouettes: Metriorhynchoidea & Teleosauroidea (c) Gareth Monger – Licence CC BY 3.0; Dyrosauridae (c) Nobu Tamura, vectorized by Zimices – Licence CC BY-SA 3.0; Crocodylia original picture (c) Thesupermart – License CC BY-SA 3.0.

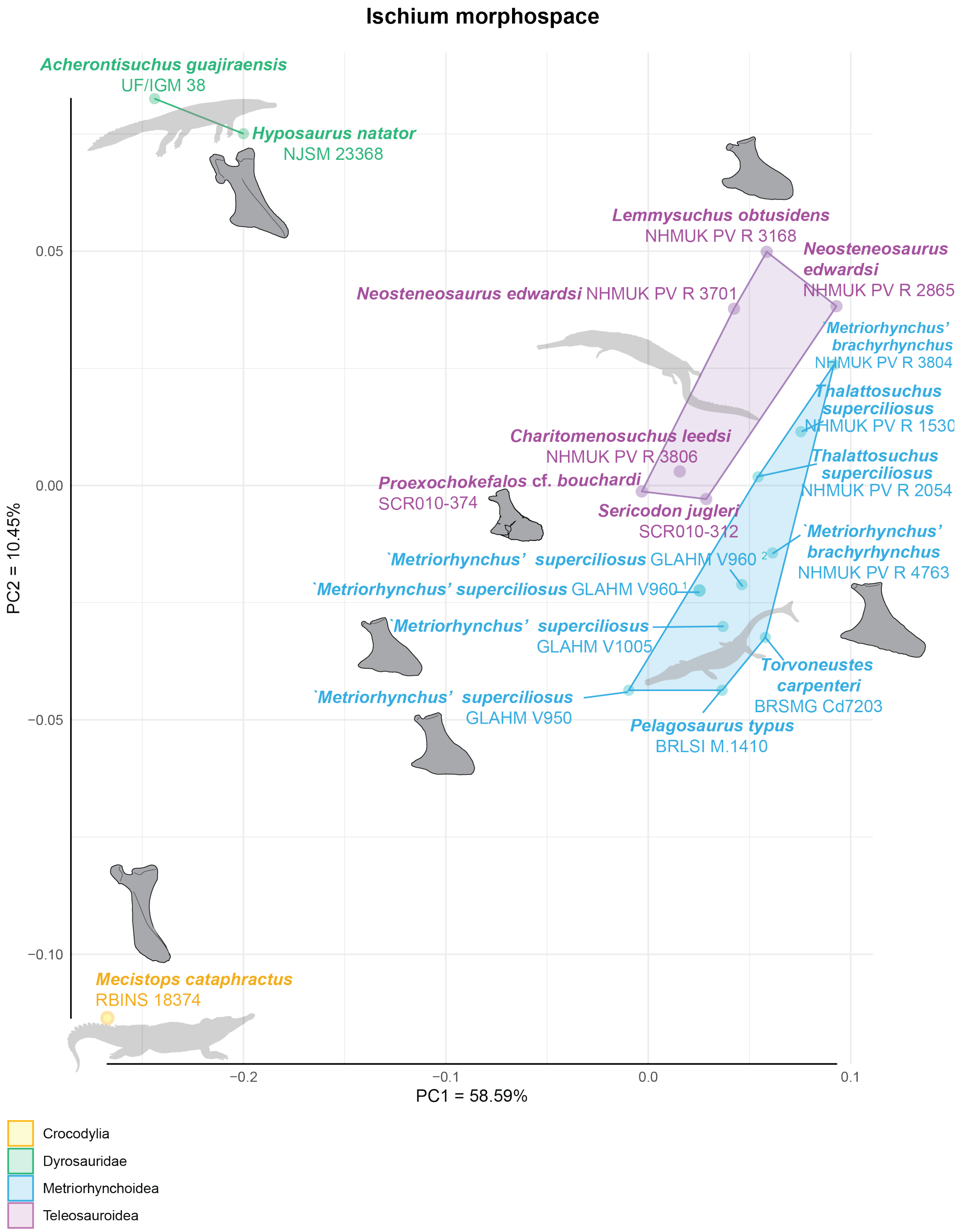

FIGURE S 28. Morphospace representing dissimilarity between the ischia of Dyrosauridea, Crocodylia, Metriorhynchoidea (Thalattosuchia) and Teleosauroidea (Thalattosuchia) using the first two PCA axes. Crocodylomorphs silhouettes: Metriorhynchoidea & Teleosauroidea (c) Gareth Monger – Licence CC BY 3.0; Dyrosauridae (c) Nobu Tamura, vectorized by Zimices – Licence CC BY-SA 3.0; Crocodylia original picture (c) Thesupermart – License CC BY-SA 3.0.

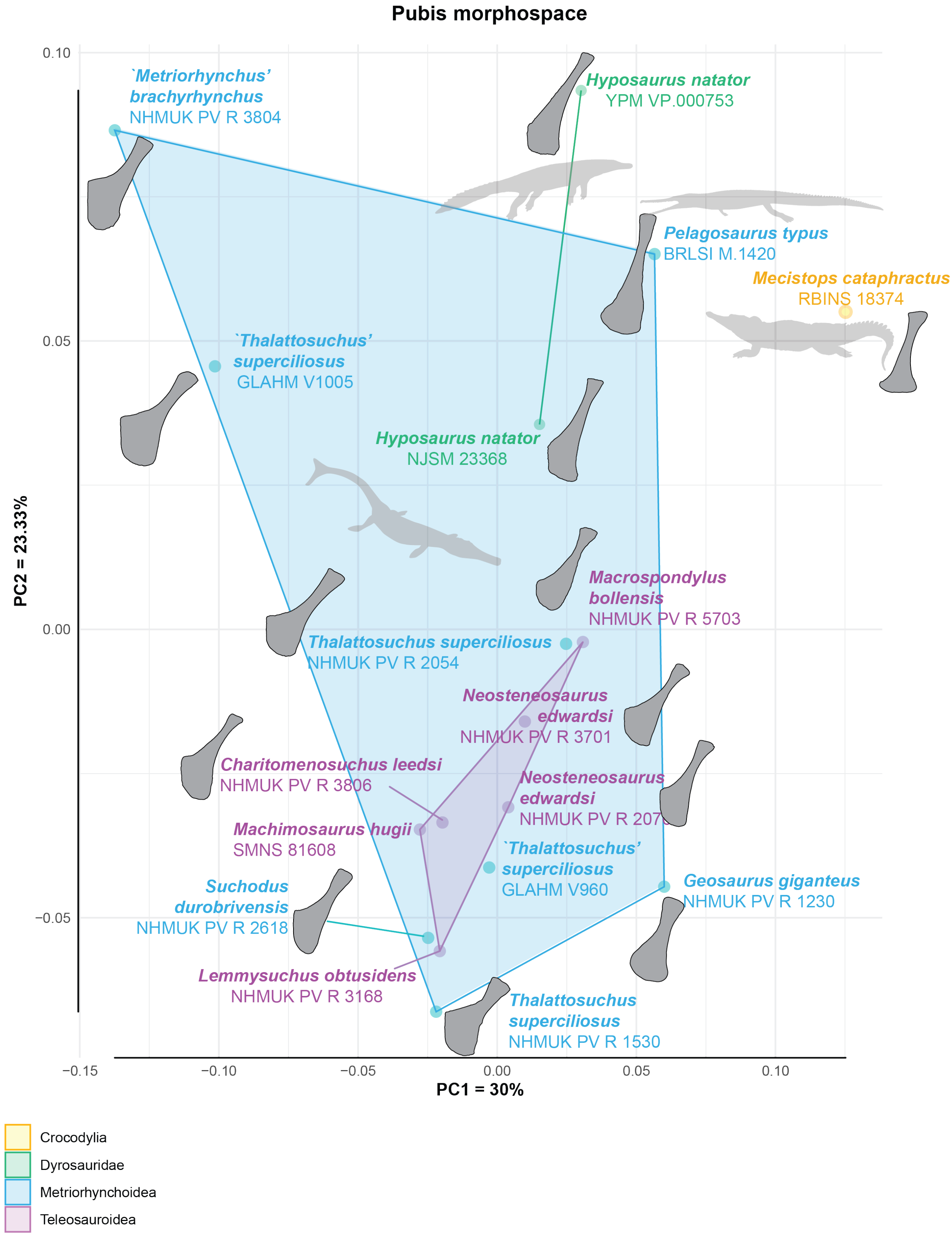

FIGURE S 29. Morphospace representing dissimilarity between the ilia of Dyrosauridea, Crocodylia, Metriorhynchoidea (Thalattosuchia) and Teleosauroidea (Thalattosuchia) using the first two PCA axes. Crocodylomorphs silhouettes: Metriorhynchoidea & Teleosauroidea (c) Gareth Monger – Licence CC BY 3.0; Dyrosauridae (c) Nobu Tamura, vectorized by Zimices – Licence CC BY-SA 3.0; Crocodylia original picture (c) Thesupermart – License CC BY-SA 3.0.

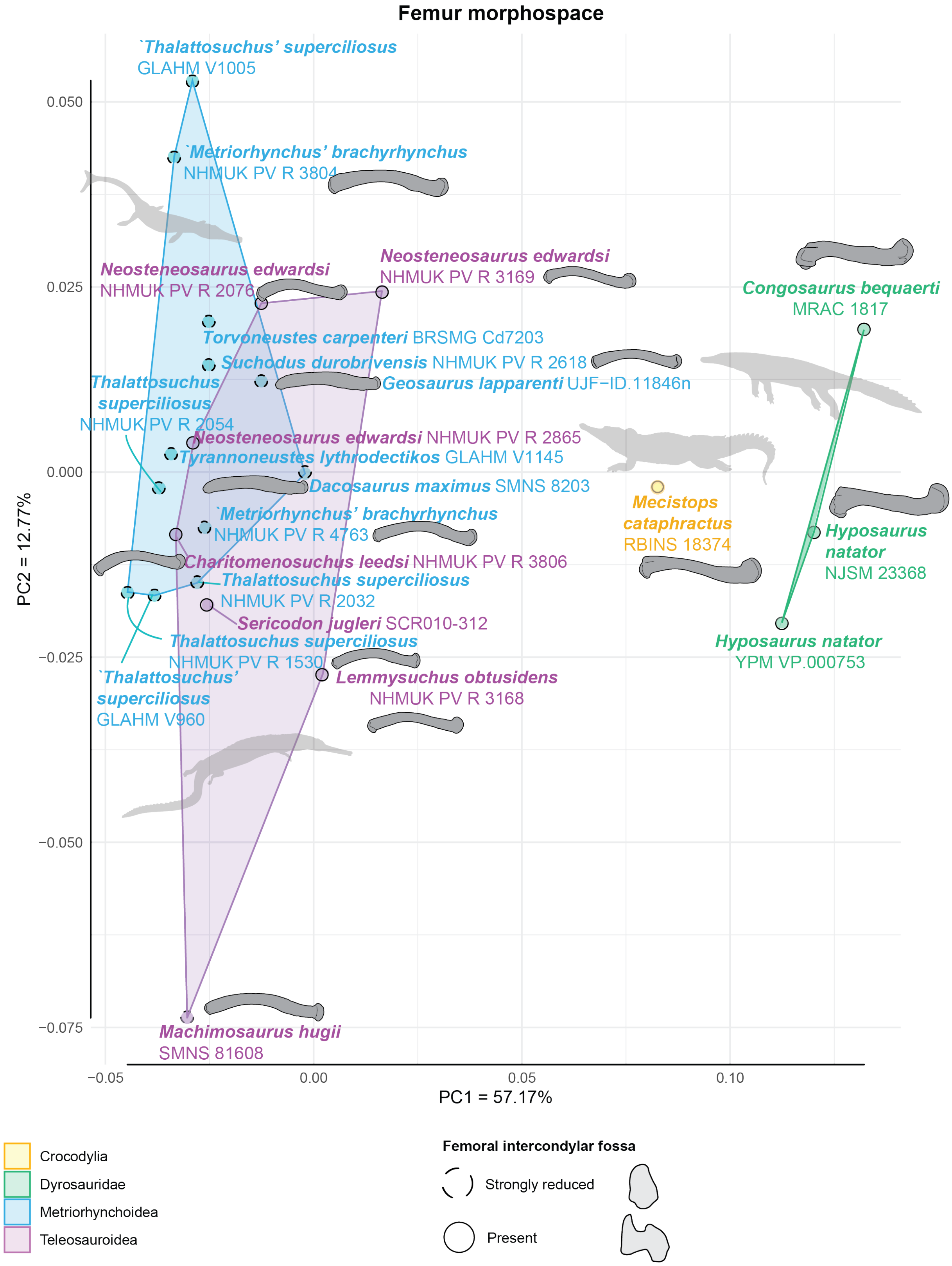

FIGURE S 30. Morphospace representing dissimilarity between the femora of Dyrosauridea, Crocodylia, Metriorhynchoidea (Thalattosuchia) and Teleosauroidea (Thalattosuchia) using the first two PCA axes. Crocodylomorphs silhouettes: Metriorhynchoidea & Teleosauroidea (c) Gareth Monger – Licence CC BY 3.0; Dyrosauridae (c) Nobu Tamura, vectorized by Zimices – Licence CC BY-SA 3.0; Crocodylia original picture (c) Thesupermart – License CC BY-SA 3.0.

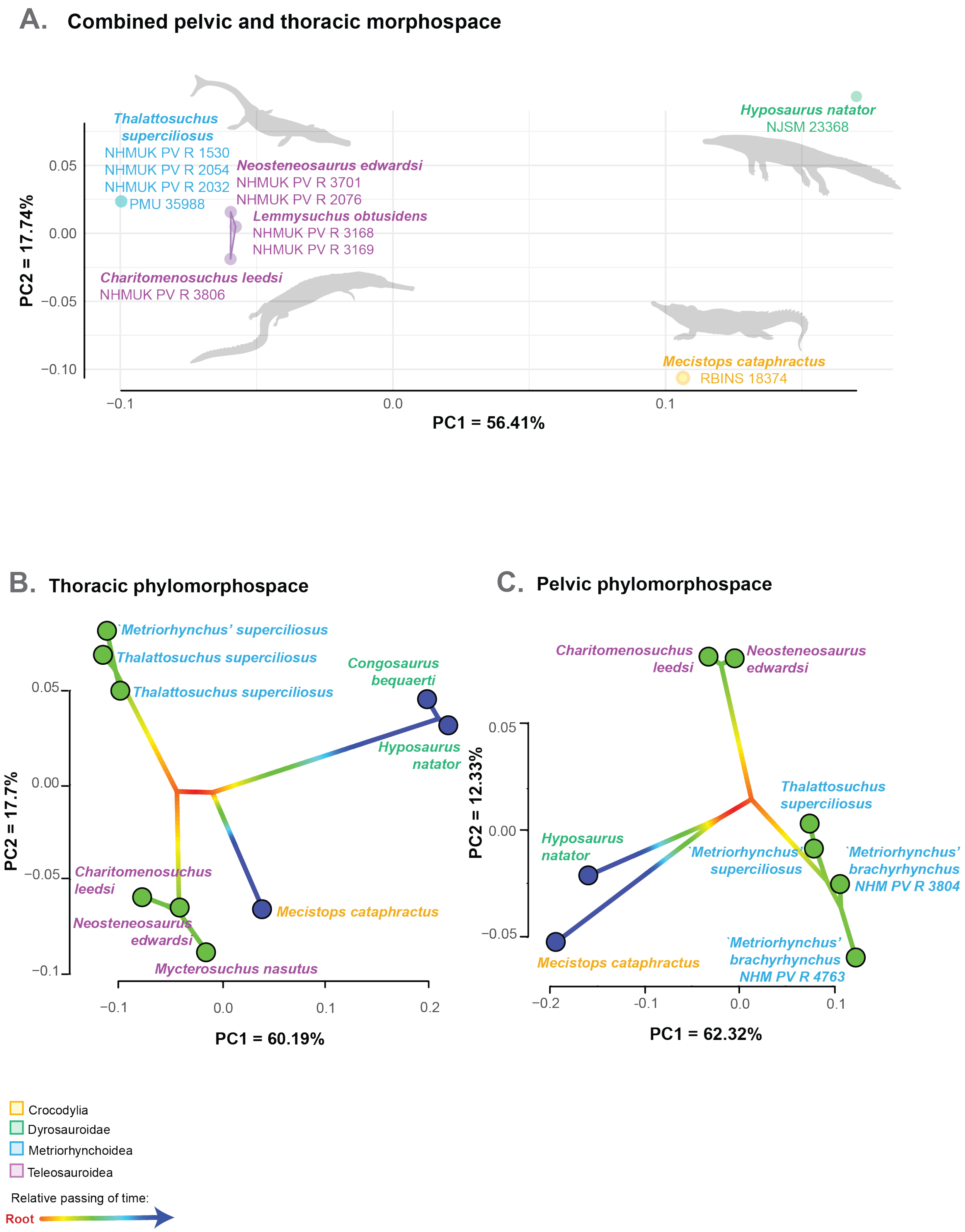

FIGURE S 31. Morphospaces representing dissimilarity between Dyrosauridea, Crocodylia, Metriorhynchoidea (Thalattosuchia) and Teleosauroidea (Thalattosuchia) using the first two PCA axes. **A.** morphospace based on the combination of pelvic and thoracic landmarks. **B.** Phylomorphospace of the thoracic combined dataset using the first two PCoA axes. **C.** Phylomorphospace of the pelvic combined dataset using the first two PCoA axes. Colored lines in phylomorphospace represent the relative passing of time since the shared root of Thalattosuchia, Dyrosauridea and Crocodylia. Hypothetical age for root based on Jouve and Jalil [2020]. Taxon ages obtained from https://paleobiodb.org. Crocodylomorphs silhouettes: Metriorhynchoidea & Teleosauroidea (c) Gareth Monger – Licence CC BY 3.0; Dyrosauridae (c) Nobu Tamura, vectorized by Zimices – Licence CC BY-SA 3.0; Crocodylia original picture (c) Thesupermart – License CC BY-SA 3.0.

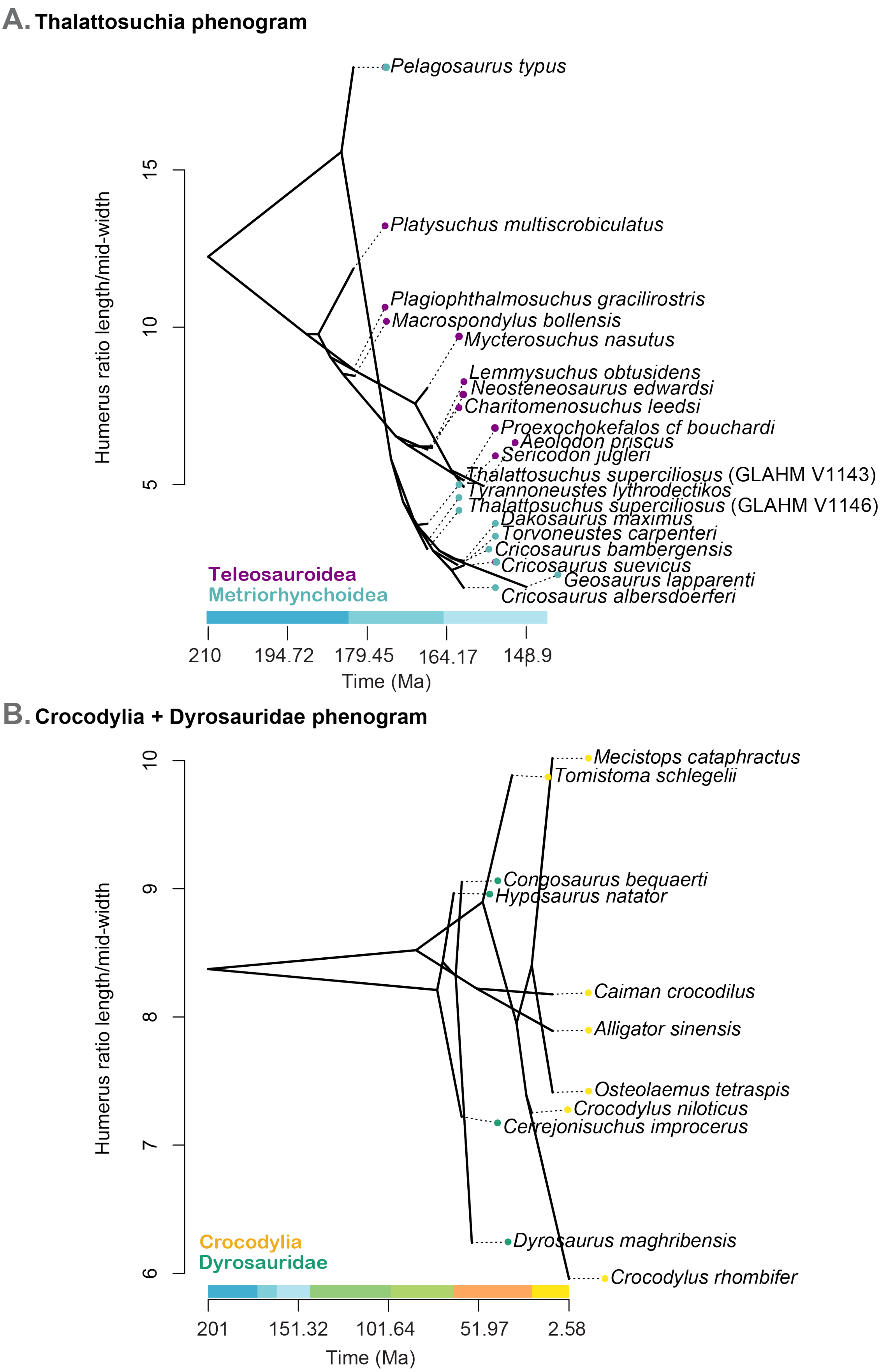

FIGURE S 32. Crocodyliformes phenograms representing the evolution of the humeral ratio. **A.** Thalattosuchia **B.**Crocodylia + Dyrosauridea. Hypothetical age for root based on Jouve and Jalil [2020]. Taxon ages obtained from https://paleobiodb.org.

Taxa	Inventory number	Hl	Hw	Ratio
Alligator sinensis	NHMW 37 966	110.07	13.95	7.89
Caiman crocodilus	NHMW 30 900	100.57	12.30	8.18
Mecistops cataphractus	RBINS 18374	111.60	11.14	10.02
Osteolaemus tetraspis	NHMW 39338:2	94.94	12.81	7.41
Crocodylus niloticus	NHMW 31.137	180.00	24.82	7.25
Crocodylus rhombifer	AMNH FARB 16697	278.00	46.66	5.96
Tomistoma schlegelii	NHMW 15626	215.00	21.75	9.89
Cerrejonisuchus improcerus	UF/IGM 31	146.80	20.33	7.22
Congosaurus bequaerti	MRAC 1741	288.73	31.89	9.05
Dyrosaurus maghribensis	OCP DEK-GE XX	418.28	67.06	6.24
Hyposaurus natator	NJSM 23368	188.00	20.97	8.97
Cricosaurus albersdoerferi	BMMS-BK 1-2	36.03	20.86	1.73
Cricosaurus bambergensis	NKMB-P-Watt14/274	23.80	9.69	2.46
Cricosaurus suevicus	SMNS9808	32.27	13.26	2.43
Dacosaurus maximus	SMNS 8203	140.44	54.47	2.58
Geosaurus lapparenti	UJF-ID11846	118.63	67.63	1.75
Macrospondylus bollensis	SMNS 9428	110.19	13.03	8.46
Pelagosaurus typus	BRLSI M.1418A	18.68	1.02	18.26
Thalattosuchus superciliosus	GLAHM V1143	64.38	17.16	3.75
Thalattosuchus superciliosus	GLAHM V1146	83.86	28.42	2.95
Torvoneustes carpenteri	Cd7203	111.61	44.54	2.51
Tyrannoneustes lythrodectikos	GLAHM V1145	89.58	27.98	3.20
Charitomenosuchus leedsi	NHMUK PV R 3806	128.39	20.99	6.12
Lemmysuchus obtusidens	NHMUK PV R 3168	193.00	31.09	6.21
Mycterosuchus nasutus	NHMUK PV R 2617	209.30	25.94	8.07
Neosteneosaurus edwardsi	NHMUK PV R 3701	122.46	19.85	6.17
Plagiophtalmosuchus gracilirostris	NHMUK PV OR 14792	128.46	14.83	8.66
Platysuchus multiscrobiculatus	SMNS9930	142.24	11.99	11.86
Proexochokefalos cf. bouchardi	MJSN SCR010-374	139.96	27.25	5.14
Sericodon jugleri	MJSN SCR010-312	104.76	21.24	4.93
Aeolodon priscus	MNHN.F.CNJ 78	86.94	17.55	4.95

TABLE S 9. List of taxa and their measurements used in the phenogram analyses. Humerus length (Hl) is taken proximodistally whereas humerus width (Hw) is taken anteroposteriorly at mid length. All measurements are in mm.

REFERENCES

S. Hua and V. De Buffrenil. Bone histology as a clue in the interpretation of functional adaptations in the Thalattosuchia (Reptilia, Crocodylia). *Journal of Vertebrate Paleontology*, 16(4):703–717, Dec. 1996. ISSN 0272-4634. doi: 10.1080/02724634.1996.10011359.

M. M. Johnson, M. T. Young, and S. L. Brusatte. The phylogenetics of Teleosauroidea (Crocodylomorpha, Thalattosuchia) and implications for their ecology and evolution. *PeerJ*, 8:1–157, 2020. doi: 10.7717/peerj.9808.

S. Jouve and N. E. Jalil. Paleocene resurrection of a crocodylomorph taxon: Biotic crises, climatic and sea level fluctuations. *Gondwana Research*, 85:1–18, 2020. ISSN 1342937X. doi: 10.1016/j.gr.2020.03.010.

E. W. Wilberg, P. L. Godoy, E. F. Griffiths, A. H. Turner, and R. B. J. Benson. A new early diverging thalattosuchian (Crocodylomorpha) from the Early Jurassic (Pliensbachian) of Dorset, U.K. and implications for the origin and evolution of the group. *Journal of Vertebrate Paleontology*, 42(3):24, Jan.

2023. ISSN 0272-4634, 1937-2809. doi: 10.1080/02724634.2022.2161909.

M. T. Young, A. Brignon, S. Sachs, J. J. Hornung, D. Foffa, J. J. N. Kitson, M. M. Johnson, and L. Steel. Cutting the Gordian knot: A historical and taxonomic revision of the Jurassic crocodylomorph *Metriorhynchus*. *Zoological Journal of the Linnean Society*, 192(2):510–553, 2020. ISSN 0024-4082. doi: 10.1093/zoolinnean/zlaa092.